TOPICAL REVIEW • OPEN ACCESS

Static theoretical investigations of organic redox active materials for redox flow batteries

Progress in Energy

TOPICAL REVIEW

Static theoretical investigations of organic redox active materials for redox flow batteries

Aleksandr Zaichenko[1,2], Andreas J Achazi[1,2], Simon Kunz[1,2], Hermann A Wegner[2,3], Jürgen Janek[1,2] and Doreen Mollenhauer[1,2,*]

[1] Institute of Physical Chemistry, Justus Liebig University, Giessen, Germany
[2] Center for Materials Research, Justus Liebig University, Giessen, Germany
[3] Institute for Organic Chemistry, Justus Liebig University, Giessen, Germany
[*] Author to whom any correspondence should be addressed.

E-mail: Doreen.Mollenhauer@phys.chemie.uni-giessen.de

Keywords: redox-flow battery, redox active molecules, molecular design, quantum chemistry, DFT, screening

OPEN ACCESS

RECEIVED
23 February 2023

REVISED
24 August 2023

ACCEPTED FOR PUBLICATION
2 November 2023

PUBLISHED
8 December 2023

Abstract

New efficient redox flow batteries (RFBs) are currently of great interest for large-scale storage of renewable energy. Further development requires the improvement of the redox active materials. Quantum chemical calculations allow the screening of large numbers of redox active molecules for required static molecular properties. In particular, redox potentials are calculated in high-throughput studies. In addition, calculations of solubility and reactivity and in-depth electronic structure analysis are performed for smaller numbers of molecules. In this review, we provide an overview of the static theoretical investigations carried out on the known classes of molecules that are considered as redox active materials in RFBs. We will focus on electronic structure methods such as density functional theory and wave function-based methods. Furthermore, investigations using the increasingly important machine learning techniques are presented. For each class of redox active molecules considered, significant theoretical results are presented and discussed. In addition, the different quantum chemical approaches used are examined, in particular with regard to their advantages and limitations. Another focus of this review is the comparison of theoretically predicted results with available experimental studies. Finally, future challenges and trends in the theoretical studies of redox active materials are highlighted.

1. Introduction

The economic need for 'green' energy is driving investment in renewable and environmentally friendly energy sources such as solar and wind energy [1]. Current international conflicts are accelerating this transition as many countries begin to strive for energy self-sufficiency [2]. Local energy production and storage would also have a positive impact on the social and economic development [3]. The social impact is particularly strong for small-scale local energy production through photovoltaics [4].

One of the main problems with renewable energy sources is their volatility (seasonal and daily changes in solar radiation, wind, etc). Therefore, the energy produced needs to be stored during periods of high output in order to be available during periods of low output [5]. A switch to renewable energy will only be possible with suitable energy storage solutions [6]. First, the energy storage solutions need to be cost effective. Second, they need to vary in size to cover everything from solar panels on a single-family home to industrial power generation. From this point of view, redox flow batteries (RFBs) have great potential because their power and capacity are independently scalable [7–9].

Historically, the first RFBs were based on reactions between transition metal ions in different oxidation states, such as vanadium or chromium. These batteries utilized V^{3+}/V^{2+} or Cr^{3+}/Cr^{2+} on the negative electrode (anode) side and VO_2^+/VO^{2+} or Cr^{3+}/CrO_4^{2-} on the positive electrode (cathode) side in aqueous solution under acidic conditions [10]. However, due to the cost and toxicity of these transition metals, there is increasing interest in organic redox active materials for RFBs. Aqueous RFBs with organic (redox) active

materials are of particular interest because they are potentially more environmentally friendly than systems based on transition metal compounds [11]. Furthermore, the organic components may be synthesized from renewable resources in the long term [12, 13].

A number of different classes of organic materials are currently explored for use as redox active materials in the two liquid phases (anolyte and catholyte) of RFBs. Besides organic molecules, organometallic complexes have great potential. The properties of both can be altered by chemical modification of the organic molecules. An important part of developing competitive, organic based RFBs is finding active materials with optimal properties. Redox-active materials determine the capacity and stability of the battery and thus essentially determine the parameters of the RFB. Volumetric capacity, redox potentials, cell voltage, solubility and chemical stability are such fundamental parameters that depend on the redox active materials of the RFB. Some of these parameters can be systematically studied using static theoretical methods [14, 15].

Quantum chemical investigations of organic redox molecules for RFBs have two main objectives. First, quantum chemical calculations are used to gain a deeper understanding of experimentally studied redox active materials. In this context, the geometric structure, electronic structure, and possible side reactions of the redox active materials are investigated [16]. Second, many molecules are screened for desired properties. Computational screening is an advantageous first step compared to time-consuming and expensive laboratory synthesis [16, 17]. However, it is beneficial for the computational predictions if experimental benchmark data are available for some molecules of the compound class under investigation.

Density functional theory (DFT) is usually the method of choice in these studies. With DFT, properties such as the redox potential and solubility can be predicted in a fast and reliable manner. In addition to DFT, machine learning (ML) tools are also starting to be used today. It should be noted that a large number of different types of organic compounds also give rise to a large number of electronic structures with different electronic affinities, chemical bonding types and molecular energy levels. In some cases, these cannot be accurately described by a single theoretical approach [18, 19].

This review focuses on theoretical calculations of important classes of organic redox active materials considered for potential use in RFBs [20]. We present and discuss the following classes of active materials: (1) stable organic radicals, (2) quinones, (3) nitrogen-containing redox active materials, (4) heterocycles containing nitrogen and sulphur, (5) pyrylium based systems. Besides organic molecules, organometallic complexes (6) are also included into the review. In many cases, there is an overlap between the different groups of active materials (1)–(5). Here we classify the compounds according to their electrochemical and structural properties. The basic structures of the organic redox active materials, their redox reactions, and important modifications as well as their design are discussed from a theoretical point of view. The available results from quantum chemical calculations of the geometric and electronic structures as well as the redox potentials of catholytes and anolytes are evaluated. The advantages, disadvantages, and existing problems of the presented theoretical results are discussed. Finally, a general overview of the different theoretical methods is presented. The applicability, advantages, and disadvantages of the different theoretical methods for different classes of redox-active material are discussed. An overview of the classes of redox-active molecules and properties considered, as well as the methods used in theoretical studies, is shown in figure 1.

All redox potentials presented in this review are given against the standard hydrogen electrode (SHE). If the redox potential is given against a different electrode in the original publication, then the potential was recalculated. Due to possible inconsistencies with different reference electrodes, we present the SHE values. The conversion data in table 1 were used to recalculate to SHE values.

2. Basics of organic RFBs

RFBs consist of three major technical components. The two electrolyte tanks, in which the catholyte and anolyte is stored separately, and the electrochemical cell in the core of the RFB, which is used for electrochemical conversion. The electrochemical cell consists of the two electrodes, mostly carbon felts or plates, and a separator that divides the catholyte and anolyte compartments (figure 2). The electrolytes (catholyte and anolyte) circulate between the tanks and the electrochemical cell. Catholyte and anolyte are electrolytes containing the solvated redox active materials with positive or negative potential, respectively. A supporting electrolyte is also included to increase the ionic conductivity. The redox active materials are molecules that can be reversibly oxidized and reduced during the electrochemical conversions in the RFB. The separator is usually a membrane that is permeable to the supporting electrolyte but impermeable to the redox active material. RFBs represent systems between a fuel cell and a conventional battery, allowing independent scaling of the power and capacity of the RFB. If the anolyte and catholyte contain the same active material, the system is called symmetrical [7].

Figure 1. Overview of molecular classes, properties and used methods in theoretical studies of this review.

Table 1. Conversion data for the recalculations to SHE values.

System	SHE value (mV)
Ag^+/Ag (sat., Aq.)	199 [21]
$Ag/AgNO_3$ (0.01 M, ACN)	544 [22]
Ag^+/Ag (0.1 M, ACN)	587 [23]
Hg^+/Hg (sat., Aq.)	244 [21]
Fc^+/Fc (ACN)	644 [24]
Fc^+/Fc (DMF)	694 [24]
Fc^+/Fc (DME)	754 [24]
Fc^+/Fc (THF)	804 [24]

The voltametric energy density W_V of a RFB is the product of the voltage U (difference between two half-cell redox potentials of the electrolytes) and the volumetric capacity C_V of the electrolyte, see equation (1):

$$W_V = U \cdot C_V. \tag{1}$$

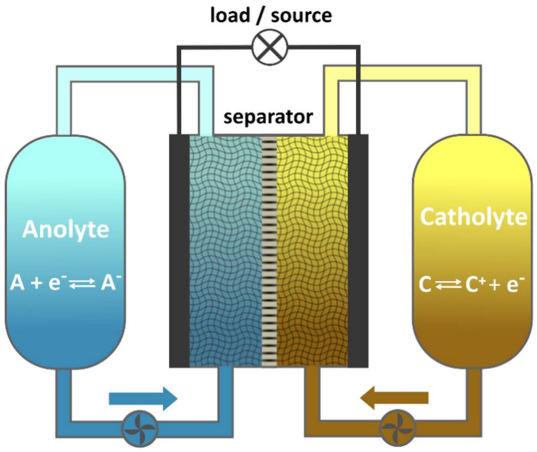

Figure 2. Schematically sketched redox-flow battery cell.

The volumetric capacity of a material depends on the solubility of the redox active molecules and the number of electrons transferred. The number of electrons transferred is specific to each electrochemical reaction. The energy density is calculated from the redox potentials and concentrations of the two active materials. The voltage is the difference between the redox potentials of the anolyte and catholyte. The redox potentials can be systematically predicted from quantum chemical calculations of the redox reactions of the redox active molecules [15]. In addition to the determination of the redox potential, the calculation of the thermodynamically stable form of reactant and product in solution is very important. These can be used to take into account different effects such as solvation of the redox active molecule, and side reactions with the solvent or the conductive salt. For example, the degree of protonation in aqueous electrolytes strongly influences the redox potential and possibly also the reactivity or stability [25].

Furthermore, kinetic parameters such as reaction rate constants, diffusion coefficients and the liquid phase thermodynamic equilibrium are important characteristics for RFBs as they influence the resulting power. However, calculating them from first principles requires computationally demanding approaches such as *ab initio* molecular dynamics simulations, the Monte-Carlo method [26], or the calculation of potential energy surfaces (PESs) and transition states according to Marcus theory [27–29]. The theoretically reliable and fast predictable properties of the model systems address important practical parameters of RFBs but are of course not a description of the real battery as a whole.

The three basic efficiency parameters of an RFB experimentally used are the Coulomb efficiency η_C, the voltage efficiency η_V, and the energy efficiency η_E. The first two denote the ratio between charge and discharge capacities and voltages, respectively, while η_E is their product [7]. Typical η_E values for RFBs range from 50% to 90% [30]. These parameters are experimentally determined and usually show the deviation from the 'ideal' theoretically predicted voltages and capacities. Compared to Li ion batteries, RFBs typically have a lower voltametric energy density in the order of 20–50 Wh l^{-1} [31]. However, the storage of the redox active material in the liquid phase in separate reservoirs leads to an advantage in scalability and the unique properties of these systems, which makes them particularly attractive as large-scale energy storage devices for renewable energy sources. The liquid state of the redox active materials also allows the use of various colloidal systems such as sols and emulsions in electrolytes, which provide technological flexibility [32, 33]. Quantum chemical modeling of colloidal systems is much more difficult and time-consuming due to the system size and environmental effects [17, 34]. Therefore, the present review focuses on single molecules in solutions as redox-active materials.

3. Theoretical calculation of the properties of organic redox-active materials

3.1. General overview of organic redox-active materials

An important advantage of organic molecules as redox active materials or as a part of a redox active system is that their properties can be tailored. Solubility, kinetic properties, and redox potentials can be adjusted by modifying the basic organic structure, for example by introducing certain functional groups [35, 36]. This allows the properties of organic RFBs to be controlled and tuned.

Aprotic or protic organic liquids as well as water are of interest as solvents for the redox active materials. Aprotic organic solvents have better electrochemical stability and a larger potential window than protic solvents [37]. With these solvents, organic RFBs can be constructed with higher energy densities than in

aqueous systems because redox couples with higher voltage differences can be utilized. However, the ionic conductivity in organic solvents is much lower than in aqueous solutions, which limits the applicable current densities [7]. Aqueous electrolytes are potentially more environmentally friendly [11] than organic ones and are associated with lower costs, rendering them particular interesting in current research [30]. The lower cell voltage and therefore energy density of aqueous systems can be overcome in stationary RFB applications by increasing the volume of the electrolyte [38]. In addition, aqueous systems usually have higher conductivity than aprotic organic systems, and by this a higher power density [7].

A typical disadvantage of organic active materials compared to metal ion based RFBs is the limited long-term stability of the electrolytes. Side reactions of the organic molecules lead to the degradation of the active material and thus to the ageing of the electrolytes, which is one of the major problems of organic RFBs [30, 39].

In the following chapters, we will first present, evaluate and classify the commonly used quantum chemical methods for theoretical investigations of organic redox-active materials. Then, the most promising classes of organic redox-active materials, for which theoretical calculations have also been carried out, are discussed. For each class considered, the best-known and most representative examples are presented.

3.2. Calculating properties of organic redox active materials

3.2.1. Theoretical calculation of the redox potential

In the first step of molecular engineering and design, candidates for organic redox-active materials can be systematically predicted *in silico* using methods from quantum chemistry. Quantum chemistry offers a variety of computational methods and approaches for *ab initio* and first principles studies of redox active materials. Artificial intelligence (AI) and ML can also be used to predict molecular properties. The training sets for AI and ML can in turn be calculated using quantum chemical methods. Ghule *et al* showed that these approaches can be used to calculate molecular properties with similar accuracy to quantum chemical calculations, but in much less time [40]. Only recently have researchers begun to apply ML tools for the investigation of redox active materials. The corresponding publications are highlighted in this review, but so far, the majority of investigations utilize quantum chemical methods.

The computational methodology for studying redox active materials by quantum chemical methods typically involves three steps. First, a molecular model system is constructed with a given number of atoms arranged in a guess for the minimum energy structure. Second, the total electronic energy of the system is calculated using one of the methods discussed in the next chapter, optimizing the structure until the minimum energy is reached. Finally, the free energy is calculated, taking into account temperature, concentration, and vibrational and rotational degrees of freedom.

The choice of the appropriate model system is a crucial step in this process. Considerations such as the chemical state of the molecules under specific external conditions and effects such as protonation, and isomerization must be taken into account. The model system should reflect the most realistic structure of the system being studied under the given conditions. If multiple conformers of the molecules are present in solution, these may also need to be considered. Typically, the redox potential based on the Gibbs free energy, the solubility expressed by the Gibbs free energy of solvation, and the stability by considering side reactions or descriptors are calculated by quantum chemical calculations [41]. From these data, general statements for the design of the redox active molecule are then identified. Furthermore, novel redox active materials can be predicted. Other possible reference parameters of the redox properties are energies of the highest occupied molecular orbitals (HOMOs) and lowest unoccupied molecular orbitals (LUMOs), or ionization energies and electron affinities [19, 42–45]. A detailed review of calculations for electrochemical reactions has been published by Marenich *et al* [29]. A general equation of the standard redox potential is given by:

$$E^0 = -\frac{\Delta G_{\text{reac}}{}^0}{nF} - E^0_{\text{SHE}} \tag{2}$$

where $\Delta G_{\text{reac}}{}^0$ is the Gibbs free energy of the electrochemical reaction, F is the Faraday constant, n is the number of electrons transferred and E^0_{SHE} is the potential of the SHE.

The SHE potential in equation (2) is known and accepted by IUPAC as 4.44 ± 0.02 V at 298.15 K [46]. It should be noted that reference values of 4.05–4.42 V have been reported from different approaches [29]. For quantum chemical calculations, the value for E^0_{SHE} depends on which Gibbs energy of solvation of a proton was used to parameterize the implicit solvent model [47]. $E^0_{\text{SHE}} = 4.28$ V is considered by many quantum chemical studies as the accurate value for the parameterization of implicit solvent models [29, 47, 48]. This value does not include the contributions from the surface potential of water. In chemically balanced single-phase reactions these contributions cancel each other out. If the contribution of surface potential needs to be included, $E^0_{\text{SHE}} = 4.42$ V can be used [29]. Newer solvent models such as SM8 and solvation

models based on density (SMD) utilize $E^0_{SHE} = 4.28$ V. Older but still common implicit solvent models use other values such as $E^0_{SHE} = 4.47$ V for polarized continuum model (PCM) [49] and $E^0_{SHE} = 4.34$ V for SM6 [50]. For the solvent models COSMO, COSMO-RS and DCOSMO-RS the Gibbs energy of solvation of a proton has not been used for parameterization [51, 52]. Therefore, it is currently unclear which E^0_{SHE} should be applied to them. In these cases, the authors of the review recommend using $E^0_{SHE} = 4.28$ V.

Overall, pre-calculated parameters from literature such as SHE potentials, free energy of protons and electrons transferred in a reaction can be sources of error. Depending on the theoretical approach or the experimental conditions, the parameters from the literature have to be chosen carefully. The SHE potential does not affect the trends of theoretically calculated results, but it contributes to the need to obtain the absolute values of calculated parameters that can be compared to experimental results.

However, solvation Gibbs energies can also be a potential source of inaccuracy in theoretical calculations. Solvation effects are usually treated with implicit solvent models. Besides the inaccuracy of the implicit solvent model itself the correct solvation Gibbs energy of a proton is of particular importance. It not only contributes to the potentials of the SHE, which are needed to compare the results to experimental values. It is also often used indirectly to parameterize the implicit solvent model, since the experimental solvation free energies of ionic solutes are obtained with thermochemical cycles that include the solvation free energy of the proton [47]. The most commonly used experimental proton solvation free energy values in literature, based on Boltzmann statistic, are -1112.5 kJ mol^{-1} and -1098.9 kJ mol^{-1} as it was discussed by Hammerich and Speiser [47]. They correspond to redox potential of SHE with values of 4.28 V and 4.42 V, respectively. The first value is in good agreement with the previously discussed theoretical value for SM8 and SMD models and the second one includes an estimate of the surface potential contribution.

Sometimes an implicit solvent model is not sufficient and the specific inclusion of explicit solvent molecules is required. Nevertheless, it is recommended [53, 54] as best practice in quantum chemistry to avoid explicit solvent molecules wherever possible. Properties tend to converge poorly with the number of explicit solvent molecules. In addition, the structure optimizations are usually long and tedious because the explicit solvent molecules lead to a flat PES with many local minima [53, 54]. The correct inclusion of the solvation effects will differ from case to case and requires careful consideration of possible sources of error.

The calculated redox potentials are the most practical parameters for theoretical research on RFBs. They can be calculated quantum chemically quickly and usually with sufficient accuracy [55]. Furthermore, readily available laboratory measurements allow easy comparison with experiments. Due to the large number of the external model parameters involved in the calculation such as free energies or reference potentials, redox potentials are not the most reliable values for a high-precision comparison of the electronic structure of redox-active molecules in theoretical studies but are mainly relevant for practical research.

Finally, the calculations of organic redox active materials can be divided in two important directions: (1) prediction of and search for novel active materials by screening of potential redox active molecules, and (2) investigation of properties, reactivities and degradation of specific molecules of interest. Detailed theoretical investigations of organic molecules and their redox reactions in different environments with respect to their possible degradation mechanism usually require more theoretical consideration than the calculation of thermodynamic parameters such as redox potentials. The different degradation mechanisms need an assumed degradation reaction and system-specific quantum chemical modeling. The systematic theoretical research of the stability of redox-active molecules is therefore a specific and complex problem [30, 56]. In screening approaches, for example, the redox potentials of many redox active molecules are calculated, and degradation is usually not taken into account.

3.2.2. Theoretical quantum chemical methods for calculation

In this section, we briefly present some basic information about the quantum chemical approaches commonly used to investigate redox active materials. In the quantum chemical calculations, the molecules under investigation are usually considered as single molecules. Solvent effects are considered using solvent models based on the continuum approach. The quantum chemical method of choice represents the DFT, which is based on the Hohenberg–Kohn theorems and within the framework of the Kohn–Sham theory. The most problematic aspect of DFT is the unknown exchange-correlation density functional of energy, which is always approximated in the Kohn-Sham theory. The basic idea of DFT is the density functional dependence of the system energy $E[\rho]$ on the electronic density ρ. The general equation of Kohn–Sham-DFT is thus:

$$E[\rho] = T_s[\rho] + V_{ext}[\rho] + U[\rho] + V_{xc}[\rho] \tag{3}$$

where T_s is the kinetic energy of electrons, V_{ext} is the interaction of electrons with cores, U is the Coulomb interaction between the electrons and V_{xc} is the exchange and correlation interaction of the electrons. The exchange-correlation term is approximated in DFT calculations.

Typically, DFT calculations for redox active molecules are based on the gradient generalized approximated (GGA) exchange-correlation density functionals such as PBE or BP86, or hybrid density functionals such as B3LYP, using non-periodic quantum chemistry software packages. The DFT calculations are performed with double ζ basis sets, sometimes triple ζ basis sets or rarely with plane-wave basis sets. DFT calculations generally provide results with a relatively small amount of computational time for small and medium-sized molecules.

Due to their approximative nature, some of the density functionals contain systematic errors, such as delocalization errors, which cause excess charge delocalization and lead to incorrect electronic densities and molecular properties [57, 58]. In general, GGA functionals overestimate the delocalization and hybrid functionals with the exact Hartree–Fock exchange terms underestimate the delocalization [59]. Different density functionals give specific deviations and errors for different classes of compounds and computational conditions in electrochemical calculations. For example, different hybrid functionals have different accuracies for the prediction of redox potentials, and their average error varies with the size of the basis set [60, 61]. Some newly developed density functionals, such as strongly constrained and appropriately normed meta-GGA functionals, show promising results for ionization energies of atomic model systems [62], but were not yet used for the molecular systems discussed in this review.

Moreover, standard DFT calculations do not take into account or strongly underestimate medium and long-range dispersion interactions. Dispersion corrections are therefore required. There are several approaches to include these dispersion interactions in the DFT calculations. The most common approaches are the DFT-D approach of Grimme, and the van der Waals corrected density functionals (vdW-DFT) [63]. DFT-D approaches are based on distance dependent damped potentials introduced as an additive correction and are developed in several generations D2, D3 and D4. The D4 correction is the most up-to-date approach in the series and the only one that takes into account the charge of the molecule. The use of dispersion corrections or improved vdW functionals is particularly important for redox active molecules where inter- and intramolecular interactions are present [64, 65].

For large systems ($\sim$1000 atoms) [66] or when large numbers of molecules need to be investigated, semi-empirical methods and tight binding approaches are used [67]. The tight binding approaches are based on DFT but have a much lower computational cost. The idea of these methods is to use a valence-only minimal basis self-consistent approach with the electronic density parameterized for several chemical elements. Recently developed extended tight binding (xTB) methods give promising results [67]. These methods do not provide quantum chemical accuracy [68]. However, they are more precise and physically correct than classical force fields and allow the calculation of much larger systems than with DFT. In addition, they can be efficiently used for preoptimization of structures and conformational analysis.

Beyond the accuracy of electronic structure calculations, environmental effects have a very significant influence on the thermodynamics and kinetics of chemical reactions. The most important environment of active material molecules in RFBs represents the solvent. Solvation effects can be explicitly described by quantum mechanics (QM)/molecular mechanics (MM) models or by implicit solvent models. Common implicit solvent models are the conductor-like screening model (COSMO), and the PCM [19]. These models depend solely on the dielectric constant of the solvent and do not include effects depending on the solvent nature. Newer implicit solvent models such as SMD and direct COSMO-RS include terms to account for dispersion interactions and hydrogen bonding to the solvent. Nevertheless, implicit solvent models can show larger errors in the results, especially if the interactions with the first solvation shell are strong (e.g. hydrogen bonding to water molecules) [69]. Explicit solvent models with solvent molecules in the model system provide more accurate and reliable results. However, such calculations require much more computational effort and the model systems become much more complicated, as shown by Sterling and Isegava [19, 70]. Therefore, the implicit solvent models are usually used for the calculation of redox active molecules. See also section 3.2.1 for a discussion of the solvation energy of a proton.

Wave function-based methods are based on the direct solution of the time-independent Schrödinger equation with an approximated wave function Ψ of a molecule (equation (4)). Equation (4) is the most fundamental ansatz of wave function-based quantum chemical calculations, linking the wave function Ψ with the system energy E as an eigenvalue of the Hamiltonian operator $\widehat{H}$.

$$\widehat{H}\Psi = E\Psi\,. \tag{4}$$

Usually, the Hartree–Fock method is employed as s basic approximation, and the electron correlation is calculated in addition. Hartree–Fock theory-based electron correlation methods are called post-Hartree–Fock methods. The post-Hartee–Fock methods such as the coupled cluster (CC) approach, the complete active space self-consistent field (CASSCF) method or the Møller–Plesset perturbation theory, provide a more detailed description of the molecules before and after the electrochemical reactions than the

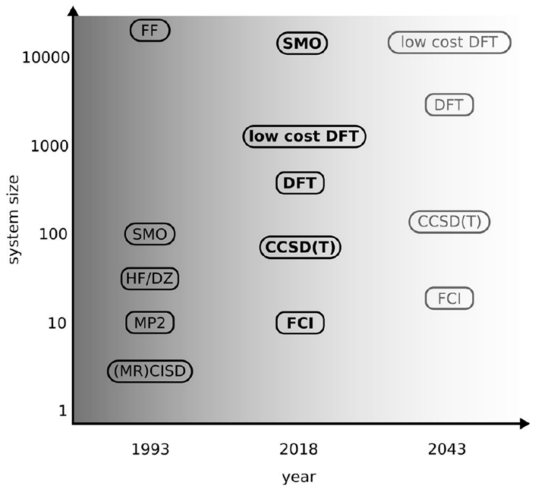

Figure 3. Electronic structure methods used for systems of various sizes that can be computed (single-point energy) on a single-core CPU within a day. Abbreviations: FF (force field), SMO (semiempirical molecular orbital), HF (Hartree-Fock), DZ (double-zeta, AO basis), CI (configuration interaction), FCI (full CI), MR (multireference), SD (single and double excitations). FCI including DMRG (density matrix renormalization group) or stochastic Monte Carlo variants. CCSD(T) here refers to accurate and controlled approximations. [76] John Wiley & Sons. [© 2018 Wiley-VCH Verlag GmbH & Co. KGaA, Weinheim].

DFT. The use of electron correlation wave function-based methods can provide very detailed information about electronic states and reaction mechanisms at the electronic transition level. The results obtained are more accurate but more constrained by the size of the model systems due to the high computational cost. In some studies considered here, redox properties calculations of selected organic and organometallic systems of limited size have been performed using the wave function based methods described [71–75].

At present, however, the post-Hartree–Fock methods are less widely applied than DFT-based methods. The higher computational complexity of the post-Hartree–Fock approach limits the size of the model system. This high computational cost also means that these methods are not suitable for large screening studies. The faster basis set convergence and the lower computational effort compared to the electron correlation methods are the well-known advantages for the preference of DFT in computational studies. In this context, the scaling factors of the computational methods (proportional to the computational effort) corresponding to the system size N are $O(N^4)$ [$O(N^3)$ with resolution of identity] for DFT, $O(N^5)$ for MP2 and $O(N^7)$ for CCSD(T).

A review with prediction of the limitations of electronic structure methods was published by Grimme and Schreiner and is illustrated in figure 3 [76].

The family of Quantum Monte–Carlo methods uses stochastic computational methods to evaluate multidimensional integrals (variational Monte–Carlo) and to find electronic states (diffusion Monte–Carlo) are used in [77]. These types of methods are very promising for accurate calculations of various molecular properties such as redox potentials, but only a few studies involve calculations of redox related properties [78–80].

In addition to the chosen theoretical methods, there are other computational details that can influence the accuracy of the results. It is important to consider factors such as basis set sizes and the specifics of the problem being investigated. The basis set superposition errors (BSSE) can also play a role, for example in the description of the intermolecular interaction of redox-active molecules (dimerization of redox active molecules) [81]. The BSSE can be significant for weakly interacting molecules and using a small basis set. Unrestricted calculations may suffer from spin contamination. Discussion of these fundamental methodological problems is beyond the scope of this review, but it is important to be aware of these methodological errors so that they can be corrected if necessary.

3.2.3. Summary of properties calculations

In summary, the standard theoretical method for ground state calculations of organic redox active molecules is DFT. It is the most universal and convincing method for screening but also degradation of different classes of active materials for RFBs [82]. However, errors in DFT calculations have been demonstrated in the modeling of some classical organic reaction mechanisms of nucleophilic addition and substitution, which are important for the description of for example degradation mechanisms and side reactions of active materials [83]. An accurate consideration of compounds such as radicals and reaction mechanisms with different spin multiplicity, symmetry breaking and spin contamination may require more expensive electron

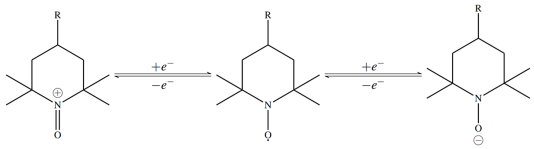

Figure 4. Reduction (right path) and oxidation (left path) of a TEMPO-based molecule (center) to the aminoxyl anion (right) and to the oxoammonium cation (left).

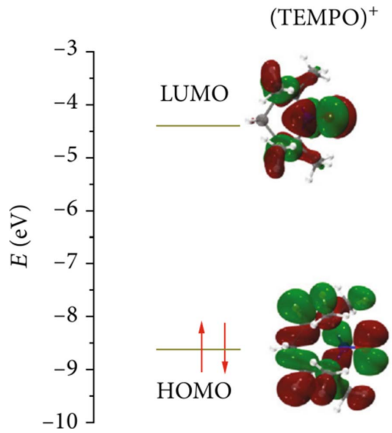

Figure 5. HOMO and LUMOs of $(TEMPO)^+$ calculated at the M062X-D3(BJ)/def2-SV (SMD solvent model of water) level of theory. Reproduced from [94]. CC BY 4.0. Color: H (white), C (grey), N (blue), O (red).

multireference correlation wave function-based methods. These are currently only rarely used for molecular design of redox active molecular materials and are more demanding than DFT calculations [84–86]. It can be concluded that there is currently no universal theoretical approach for investigating organic redox active materials in all practical cases. Each theoretical approach contains specific approximations and has specific advantages and disadvantages depending on the research case and system size.

3.3. Stable organic radicals

Radicals as organic redox active materials can be neutral molecules or ionic species. The solvent can be aqueous or non-aqueous. Typically, ionic radicals are products of electrochemical reactions following electron transfer during reduction or oxidation [87]. The class of radicals encompasses a variety of redox active materials, and this chapter discusses several typical neutral radicals with corresponding reduction and oxidation reactions and their modifications. In general, these radicals are based on cyclic systems with heteroatoms.

3.3.1. TEMPO-based radicals

The class of 2,2,6,6-tetramethylpiperidine-1-oxyls (TEMPO) is a very well-studied cathode material. Research on TEMPO in the context of RFBs has focused on finding the most suitable modification to make it suitable as a catholyte. Experimental studies exhibit many possible modifications and a great synthetic potential of the TEMPO core structure for the development of active materials. For example, the soluble molecule *N,N,N*-2,2,6,6-heptamethyl-piperidinyloxy-4-ammonium chloride was found to be an efficient electrolyte in high capacity aqueous RFBs [88–90]. TEMPO-based radicals are also used in combination with other active molecule fragments, such as phenazine, for symmetrical RFBs as a bipolar active material for both anolyte and catholyte [91].

The cathodic and anodic reactions of TEMPO-based molecules with a –R substituent and the corresponding one-electron transitions are presented in figure 4. The oxidation of the TEMPO molecule leads to the formation of an oxoammonium cation $(TEMPO)^+$ with oxidation potential $E^0 = 0.73$ V vs. SHE in water [92] (0.72 V [93]). The reduction results in the hydroxylamine anion $(TEMPO)^-$. In these processes, the single occupied molecular orbital (SOMO) becomes either the LUMO or the HOMO (figure 5). The HOMO and LUMO show a localization of the unpaired electron at the N–O molecular fragment. There is also a stronger delocalization of the energetically lower lying electron pairs in the σ-bounded ring system.

The orbitals and spin states for reduced and oxidized TEMPO were calculated and analyzed, among others by Mao *et al* for different oxidation states at the B3LYP/6-3+1G(d,p) (CPCM) level of theory [95].

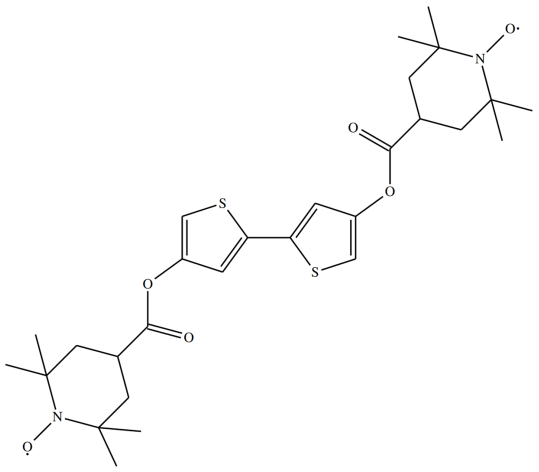

Figure 6. Example of TEMPO-thiophene based compound.

The CPCM solvent model was used to simulate methanol and acetonitrile. Calculations were performed for systems with pyridinium cationic lipid substituent. The computational results show that the functional group plays a very important role in the electronic structures and related properties of TEMPO derivatives. The TEMPO molecule converts to a singlet state after the one-electron reduction, while the substituted pyridinium lipid becomes a triplet. Calculated UV–vis spectra at the TDDFT level of theory were also provided in good agreement with the experiment and serve to interpret the spectra.

Theoretical investigations of the electrochemical properties at DFT/B3LYP and HF/MP2 levels of theory with PCM in water, DMF and ACN of TEMPO-based nitroxide radicals show a particular positive redox potential shift of the oxidation reaction with electron-withdrawing substituents R in position 4 (figure 4) [16]. The trend of these shifts is in good agreement with experimental results from the work of Mendkovich *et al* [96]. Due to the nature of the TEMPO structure without π-electron conjugation in the piperidine ring, the inductive (I) effect of substituents (–R) primarily affects the redox potentials through changes in the σ-bond electron density. For example, –H as a substituent in the basic structure of TEMPO causes a neutral inductive effect and leads to lower redox potentials than the cyano-group, oxygen-containing groups, or halogens, which show a stronger inductive withdrawing effect. These shifts are particularly observed for systems in aqueous solution. In this context, it was shown at the MP2/aug-cc-pVTZ level of theory that the Gibbs free energy ΔG_r^0 for the oxidation of the unsubstituted system in vacuum increases by more than 0.3 eV (0.3 V redox potential shift according to equation (2)) when a single –CN group is introduced. This potential shift effect was similarly observed by Hodgson *et al* for various TEMPO-based derivatives at DFT-B3LYP, MP2 and QCISD levels of theory in combination with their own n-layered integrated molecular orbital and MM' ONIOM method [97]. These calculations have been carried out in the gas phase and with the PCM model in aqueous medium. The different theoretical methods give good accuracy of redox potentials with a difference of 0.01 V from each other.

An example of DFT failure for TEMPO based structures is the calculation of charge transfer in a TEMPO-thiophene-based derivative. The results are presented in the paper of Zens *et al* [98]. The use of TDDFT to calculate PESs provides qualitatively incorrect results with incorrect energy level behavior of the PES in regions of state crossing. The use of the CASSCF method with perturbatively included dynamic correlation (NEVPT2) confirms both the strong static correlation and the importance of the dynamic correlation. Moreover, this method gives a correct result for the experimentally observed charge transfer according to the Marcus theory. The state average CASSCF method is used to correctly predict the structure reorganization. The influence of electronegative functional groups in the molecular chains between TEMPO and thiophene core on the charge transfer confirms an electron-withdrawing effect (figure 6). This effect favors the intramolecular oxidation of the TEMPO groups.

A detailed analysis of the conformers and magnetic properties of the stable TEMPO-based radical 4-amino-2,2,6,6-tetramethylpiperidine-1-oxyl-4-carboxylic acid (figure 7) in aqueous solution (PCM) and in vacuum was reported by D'Amore *et al* using the PBE0/6-31G(d) approach and the HF-based quadratic configuration model including single and double excitations. Based on the calculations, the most preferred conformational structures and Ramachandran maps were reported. Furthermore, the dependence between the conformational stability and the dielectric properties of the solvent for a given substitution pattern was demonstrated. The calculated magnetic properties agree well with experimental observations [99].

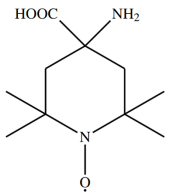

Figure 7. Molecular structure of 4-amino-2,2,6,6-tetramethylpiperidine-1-oxyl-4-carboxylic acid.

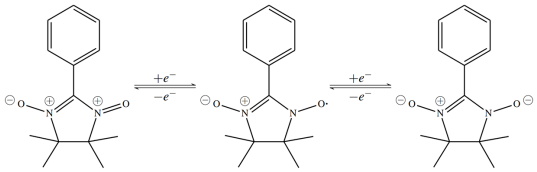

Figure 8. Reduction and oxidation of the PTIO-radical (center) to the oxoammonium cation (left) and to the aminoxyl anion (right).

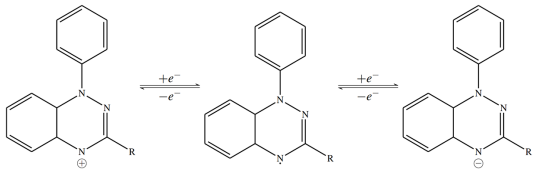

Figure 9. Reduction and oxidation of the Blatter radicals (center) to the Blatter cation (left) and the Blatter anion (right).

3.3.2. The 2-phenyl-4,4,5,5-tetramethylimidazo-line-1-oxyl oxide (PTIO) radical

The next important radical system for symmetric non-aqueous RFBs is PTIO [100–102]. The radical can be reversibly oxidized and reduced to oxoammonium and aminoxyl ions at a theoretical cell voltage of 1.73 V in acetonitrile. The reaction of the nitroxide radical group is similar to the TEMPO one-electron reduction and oxidation reactions (figure 8) [101]. Symmetric non-aqueous RFBs based on PTIO have promising efficiencies, but there is a continuous loss of capacity due to the decomposition of the active material.

Similar to TEMPO, different modifications of PTIO are possible; for example, a PTIO-based bipolar radical with various substitution patterns at the phenyl group [100]. There are currently no published theoretical results for PTIO-based systems, and calculations are expected to be challenging due to the complicated charge delocalization in the radical and the possible multi-reference character. DFT calculations may lead to an incorrect description, similar to what was demonstrated for some symmetric radical-cationic systems such as butadiene's by Oxgaard and Wiest [103]. Qualitatively different results have been reported that depend on the calculated electron localization and delocalization. Post-Hartree–Fock calculations can also be problematic for the description of PTIO-radicals due to the large size of the molecule. In addition, the instability of this radical with different ionic moieties requires a systematic consideration of side reactions and degradation processes. Therefore, the theoretical investigation of these systems represents a particularly important step, but also a challenge.

3.3.3. Blatter radicals

The electrochemistry of the 1,2,4-benzotriazin-4-yl (Blatter) radicals as a bipolar active material for the construction of RFBs was reported with symmetrical electrolyte composition with cell potentials ranging from 0.91 to 1.32 V in ACN (figure 9). The reduction and oxidation potentials for the reactions of the Blatter radical (R = Ph) are −0.60 V and 0.44 V, respectively [104]. Blatter radicals exhibit good chemical stability in all charge states, making them particularly promising active materials.

Theoretical calculations of the electronic structure of the Blatter radical have revealed a high degree of electron delocalization within the SOMO over the two conjugated ring systems (figure 10), as well as a paramagnetic character of the molecule. During the one-electron redox reactions, the SOMO converts to the LUMO in the oxidized form, and to the HOMO in the reduced form. In contrast to TEMPO, the Blatter

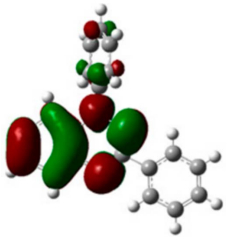

Figure 10. SOMO of the Blatter radical calculated at the UB3LYP/6-311+G(d,p) level of theory. Reproduced from [105]. CC BY 4.0. Color. Color coding: H (white), C (grey), S (yellow).

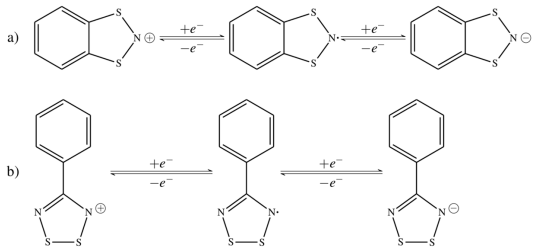

Figure 11. (a) Cathode and anode reaction of the benzo-1,3,2-dithiazolyle (B132DTA) radical: one-electron reduction to the dithiazolate anion and oxidation to the dithiazolium cation. (b) Oxidation and reduction of the 4-phenyl-1,2,3,5-dithiadiazolyle (P1235DTDA) radical: one-electron reduction to the dithiadiazolate anion and oxidation to the dithiadiazolium cation.

Table 2. Acronyms of dithiazolyle- and dithiadiazolyle- radicals.

Molecule	Acronym
4-phenyl-1,2,3,5-dithiadiazolyle	P1235DTDA
4-phenyl-1,3,2,5-dithiadiazolyle -	P1325DTDA
benzo-1,2,3-dithiazolyle	B123DTA
benzo-1,3,2-dithiazolyle	B132DTA

Table 3. Experimental redox potentials (in mV vs. SHE) of dithiazolyle- and dithiadiazolyle radical in ACN.

Molecule	Reduction potential	Oxidation potential
P1235DTDA	−586 [108]	844 [108]
P1325DTDA	—	574 [109]
B123DTA	−756 [111]	424 [111]
B132DTA	−956 [110]	394 [110]

radical is a strongly conjugated π-system with higher electron delocalisation in the radical. Therefore, we can expect stronger potential shifts from substituents with mesomeric effects [105, 106].

3.3.4. Dithiazolyle- and dithiadiazolyle-based radicals

Another group of potentially interesting systems for RFBs are radicals based on heterocyclic nitrogen-sulphur systems such as dithiazolyle- and dithiadiazolyle-based radicals (table 2) and their derivatives with different functional groups on the benzene ring and their isomers [107–111]. As with the previous radicals, these radicals can be either oxidized or reduced by a one-electron process (figure 11). The experimentally determined redox potentials of the benzo-dithiazolyle-(BDTA) and 4-phenyl-dithiadiazolyle-(PDTDA) radicals and their acronyms are given in tables 2 and 3.

Theoretical investigations of these radicals at the DFT-PBE level of theory provide reliable predictions of the redox potential without qualitative errors for the various forms of the systems. The HOMOs, SOMOs and LUMOs of cations, radicals and anions are presented in figures 12 and 13. Interestingly, due to the structural deformation, the anion exhibits an overlap between the phenyl group and the heterocyclic fragment. This is expected to result in different chemical binding properties compared to the flat structures of the cation and anion. This is particularly evident for B132DTA in figure 12.

All BDTA HOMOs contain strongly conjugated and delocalized π-systems over both rings. This leads to a significant influence of substituents with mesomeric effects. The two ring systems in PDTDA are separated

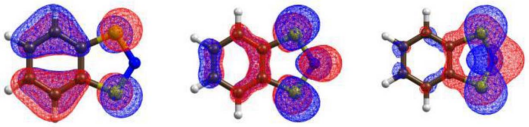

Figure 12. HOMO or SOMO of B132DTA [from left to right (oxidized, neutral, reduced)] calculate at PBE-D4/aug-cc-pVDZ (COSMO, ACN) level of theory. Visualized with a contour value of 0.03. Color code: H (grey), C (brown), N (blue), O (red), S (yellow).

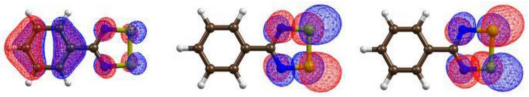

Figure 13. HOMO or SOMO of P1235DTDA [from left to right (oxidized, neutral, reduced)] calculated at PBE-D4/aug-cc-pVDZ (COSMO, ACN) level of theory. Visualized using a contour value of 0.03. Color coding: H (grey), C (brown), N (blue), O (red), S (yellow).

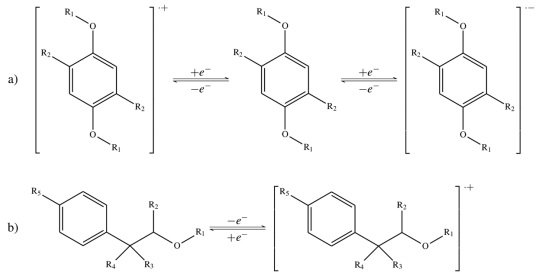

Figure 14. (a) Alkoxybenzene-based materials: reduction to anion- (right) and oxidation (left) to cation-radicals; (b) oxidation of homobenzylic ethers to cationic radicals.

by a σ-bond. Due to possible rotations and weaker π-overlap between the two ring systems, the inductive effect of the substituted phenyl group influences the redox potential. Theoretical calculations confirm the weak influence of substituents with mesomeric effect on PDTTDAs [97]. DFT-based screening studies of the PDTDAs and BDTAs radicals also show a positive influence of electron-withdrawing and -donating effects on the redox potential shift due to substitution of the benzene ring. The potential shift is particularly strong for delocalized aromatic conjugated systems of dithiazolyl radicals with conjugation of π-electron systems as seen from the orbital structure. Potential shifts are greater than 200 mV for PDTDA and greater than 500 mV for BDTA [112].

3.3.5. Aromatic compounds with ether groups

Another group of aromatic systems that are not radicals in neutral form but form ionic radicals in charged RFBs are aromatic systems with ether groups. These materials are usually based on alkoxybenzenes (figure 14(a)). The transfer of one electron by reduction or oxidation reactions produces ionic radicals with strong delocalization. These molecules are used in solution or attached to polymers, but the low energy density of some of these materials makes their application problematic. The most common core structure is 1,4-di-*tert*-butyl-2,5-dimethoxybenzene with various substituents on the ether [7, 113]. The oxidation potential of the basic structure is 1.3 V vs. SHE in ACN [114]. The effect of electron-withdrawing and electron-donating groups was demonstrated for this class of molecules in a screening approach at the B3LYP/6-31+G(d) (PCM, water) level of theory [115].

Other materials containing a benzyl group are homobenzylic ethers. Doan *et al* systematically studied 1400 homobenzylic ether derivatives in one electron oxidation reactions (figure 14(b)) [116] at the B3LYP/6-31+G(d,p) level of theory using the PCM solvent model simulating the solvent acetonitrile. The Bayesian Optimization (BO) machine-learning tool was then used to search for favorable materials and find the best structure. The research demonstrates the modern trend of using machine-learning tools in combination with quantum chemical data. Significant results were obtained from a large-scale screening of 112 000 structures analyzed by active learning. As a result, oxidation potentials of around 0.75 V were predicted, but unreliably high potentials ($\geqslant$3.5 V vs. SHE) were obtained for several electron-deficient systems with strong withdrawing substituents such as –NO_2. The unreliable results may be due to the

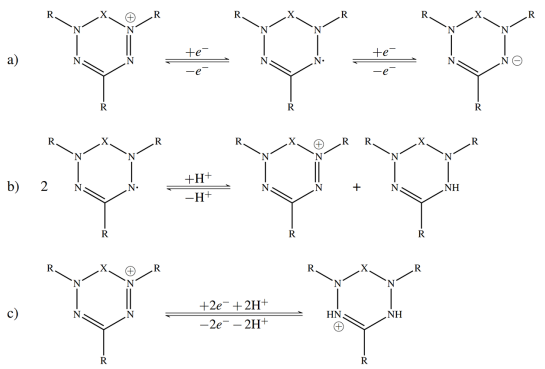

Figure 15. (a) Single electron reduction/oxidation of verdazyl species in organic electrolytes; (b) disproportionation of the verdazyl radical in acidic electrolytes; (c) electrochemical reaction of the verdazyl species in acidic electrolytes involving two electrons and two protons (R = organic substituents, X = CH_2 for (b) and (c) [120, 121], CO, CH_2 for (a) [118]).

incorrect description of nitro compounds at the DFT level of theory with a corresponding overestimation of the free energies of the reactions. Reorganization energies and the reaction energetics of deprotonation and demethylation of charged species are proposed as the theoretical relative stability criteria for this compound class [117].

3.3.6. Verdazyl radicals

Verdazyl radicals are another well-established class of stable organic radicals. The two most common variants of this class are (1) the so-called Kuhn-verdazyl radicals with X = CH_2 and (2) the oxo-verdazyl radicals with X = CO (figure 15) [118]. However, the thio-verdazyl radicals have also been reported [119].

The basic structure of the verdazyl radicals consists of a cyclic 1,2,4,5-tetrazine. Unlike other classes of stable radicals, verdazyl radicals have a sterically unprotected radical moiety [120]. The high radical stability is attributed to the delocalization of the unpaired electron between the N1–N2 and N4–N5 atoms [122]. There is no spin delocalization at the C3 positions found because the SOMO has a nodal plane there [122, 123]. Additional stabilizing resonances are obtained for the oxo- and thio-verdazyl radicals by the carbonyl and thiocarbonyl groups, respectively.

In organic electrolytes, verdazyl radicals have three redox states: the oxidized, the neutral (radical) and the reduced state (figure 15(a)). This makes them a potential candidate for symmetric organic RFBs. Cell voltages of ≈1 V (Kuhn-verdazyl radical), and ≈1.6 V (oxo-verdazyl radicals) are expected based on experiments [118]. Unfortunately, the stability of the verdazyl radicals is not yet satisfactory. The capacity rapidly faded in symmetrical batteries over 50 cycles (Kuhn-verdazyl radical) [124] and 150 cycles (oxo-verdazyl radical) [125], respectively. While the reduced form was speculated to be responsible for the degradation in battery tests [124], a recent study by Steen *et al* attributes this to decomposition of the verdazyl radical [126]. In aqueous acidic electrolytes, the verdazyl radical shows a very different behaviour. The verdazyl radical disproportionates into the oxidized (verdazyl cation) and reduced (leuco-verdazyl) states (figure 15(b)) [120]. A first detailed study of the verdazyl species after this disproportionation was recently performed by Kunz *et al* [121]. It was shown that the reversible redox reaction from the oxidized to the reduced species, is a single reaction involving two electrons as well as two protons (figure 15(c)). At pH = 0, the midpoint potential of the redox reaction is 0.146 V vs. SHE. Furthermore, the redox reaction has a large rate constant ($k_0 \approx 2 \times 10^{-2}$ cm s^{-1}) compared to other organic compounds that are discussed as potential redox active materials. The one-step reaction process means that the acidic verdazyl solutions cannot be used for symmetrical RFBs. However, the ability to store two electrons, the use of aqueous electrolytes, and the fast reaction kinetics are currently motivating further research into electrochemistry of verdazyl species in aqueous acidic electrolytes.

Koivisto and Hicks [122] speculated that the lack of spin density at the C3 group would dampen the effect of substituents at C3 on the spin distribution. However, a combined experimental and theoretical study by Tanaseichuk *et al* [123] showed that substituents at C3 have strong effects on the SOMO energy and reaction barriers. The calculations were performed at B3LYP/6-31G(d) level of theory and focused on the determination of orbital energies and spin densities. The reaction pathway of the thermolysis of the verdazyl radical in organic electrolytes was further unraveled by Steen *et al* [126] using DFT calculations. The reaction pathway was calculated at the B3LYP/def2-TZVP level of theory. The solvent (ACN) was simulated with the SMD model in subsequent single point calculations. The results were verified by experimental NMR studies.

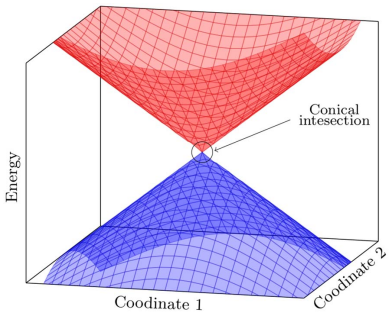

Figure 16. Schematic illustration of a conical intersection in a system.

It was found that the verdazyl radical forms a leuco-verdazyl by removing a proton from another verdazyl radical. The second verdazyl radical transforms irreversibly into an 1,2,4-triazole.

Theoretical investigations were also carried out by Kunz *et al* [121] to gain further insight into the thermodynamics and protonation sites of the verdazyl in aqueous acidic electrolytes. A protonation site screening was performed by combining the semiempirical tight binding method xTB (GFN2-xTB) in the CREST program package with DFT. The DFT calculations were performed at the B3LYP-D4/def2-TZVPD COSMO level of theory with COSMO simulating water. The pH-value was included by adding a proton concentration dependence on the correction of the Gibbs energy of the proton. Furthermore, the thermodynamics of the disproportionation of the verdazly radical in water was calculated (figure 15(b)). It was shown that disproportionation into the oxidized and reduced verdazyl species is only possible at low pH-values.

3.3.7. Summary of theoretical studies of radicals for RFBs

Stable organic radicals represent a large and diverse class of molecular compounds with potential as redox active materials for RFBs. The systematic theoretical consideration of radicals in the ground state and in redox reactions has in most cases been successfully carried out at the DFT level of theory and in agreement with experimental results of redox potentials, solvation and magnetic properties [96, 97, 99, 106]. However, the results require careful analysis and interpretation of the electronic structure and states. Open shell restricted and unrestricted methods were used in the calculations discussed. For most systems, DFT with PBE or B3LYP density functionals provide results with an accuracy comparable to post-Hartree–Fock methods. When using unrestricted methods, spin contamination is a possible source of potential problems associated with the correct description of the electronic structure. For the investigation of reaction mechanisms with conical intersections of PESs including excited states (figure 16) and systems with multi-reference ground states, the description by single reference methods such as Kohn–Sham DFT becomes problematic. In these cases, possible errors in spin state definitions, incorrect electronic structure predictions and reaction energy errors are expected [98]. Only some specific types of density functionals with exact exchange can correctly describe such situations in model systems as presented in the work of Liu for simple diatomic systems [127, 128].

In addition, DFT is known to be deficient in the description of radical reactions, even compared to the MP2 method, and this can be critical for investigations of side reactions and degradation [129]. Different types of electron correlations lead to inconsistent results for different molecules and complicate the description of reactions such as degradation mechanisms, and the calculation of experimentally measurable observables such as optical spectra at the commonly used DFT/PBE and DFT/B3LYP levels of theory. The use of wave function based multi-reference methods based on Hartree-Fock or in combination with DFT is problematic due to the system size. However, it is applicable to potentially interesting molecules of limited size or model systems. Typically these molecules are not larger than a few tens of atoms (figure 3) and the size of the active orbital space is not larger than 16 with a corresponding number of reference wave function configurations as discussed in the review by Szalay *et al* [130, 131]. Differences in method efficiency may become a major challenge for future screening research with large structural diversity, as there is no universal theoretical method for all types of systems and all research questions.

3.4. Quinones

The first reported organic redox active materials for RFBs were quinone derivatives [7, 132, 133]. Quinones are used in aqueous and non-aqueous electrolytes [31, 134, 135]. The reduction reaction of a quinone in

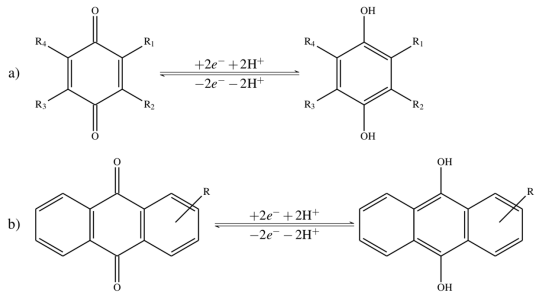

Figure 17. (a) Reduction of a benzoquinone via a two-electron and two-proton transfer in aqueous acidic solution to a hydroquinone. (b) Reduction reaction of the anthraquinone basic structure via a two-electron and two-proton transfer in aqueous acidic solution to a 9,10-dihydroxyanthracene.

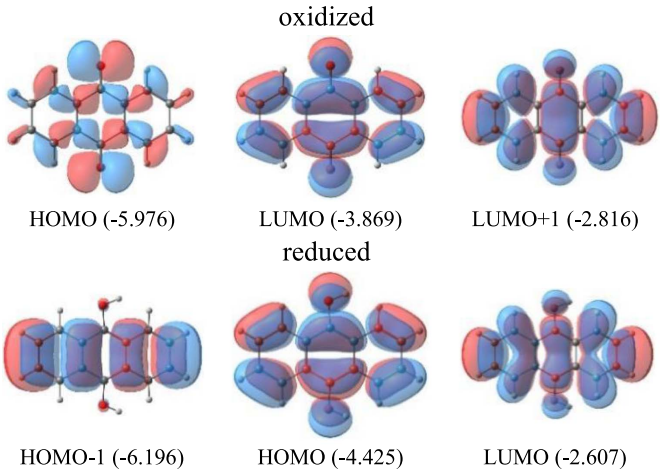

Figure 18. HOMOs and LUMOs of anthraquinone calculated at the PBE-D3BJ/aug-cc-pVDZ level of theory. (Isodensity value = 0.0145) The orbital energies are given in brackets in eV [141]. Color coding: H (white), C (grey), O (red).

aqueous medium occurs with a two-electron and two-proton transfer under acidic conditions (figure 17(a)). Hence, the arising aromatic conjugation in the benzene ring of the product stabilizes the system [134, 135]. There is a large class of quinone-based redox active materials for RFBs with different carbon basis structures [136, 137]. The first compound in this series is the benzoquinone with substituents $R_1 = R_2 = R_3 = R_4 = H$, while the best studied redox-active materials are the anthraquinones (figure 17(b)) [138].

The orbital representation of the electronic structure exhibits a shift of HOMOs and LUMOs after electron transfer. The LUMO of the quinone becomes the HOMO of the dianion and stabilizes the bonds in the aromatic structure. The HOMO of the oxidized form does not change to become an energetically lower lying orbital in the reduced form. The LUMO+1 of the oxidized form remains the LUMO of the reduced form (figure 18) [139–141]. The electronic structure of the orbitals in figure 21 suggests a strong electronic delocalization in the aromatic framework.

The unsubstituted anthraquinone core structure as an anolyte has relatively low reduction potentials of −0.68 and −1.43 V (vs. SHE) in DMF [142]. Anthraquinone-2,6-disulfonate in aqueous solution with 1 M H_2SO_4 has a reduction potential of 0.21 V vs. SHE [132]. The first reduction step in non-aqueous solution produces the anion-radical. Nevertheless, it is possible to synthetically modify this class of compounds to vary the properties such as the redox potentials or solubility [143, 144]. Solubility in water is usually controlled with polar active Brønsted acic groups such as $–SO_3H$ [145–147].

Theoretical calculations of the electrochemical properties of benzoquinone in acidic environment have been performed at the B3LYP(PCM, water)/6-31+G(d,p) level of theory. The electrostatic potential maps (EPM) contours presented in the investigations show that the most likely sites for nucleophilic reactions on carbon atoms are near electronegative atoms such as oxygen. The molecular orbital energies and HOMO-LUMO gaps indicate trends in the electrochemical behaviour of molecules in reduction and oxidation reactions. There is a tendency for the redox potentials of the molecules to decrease linearly with the

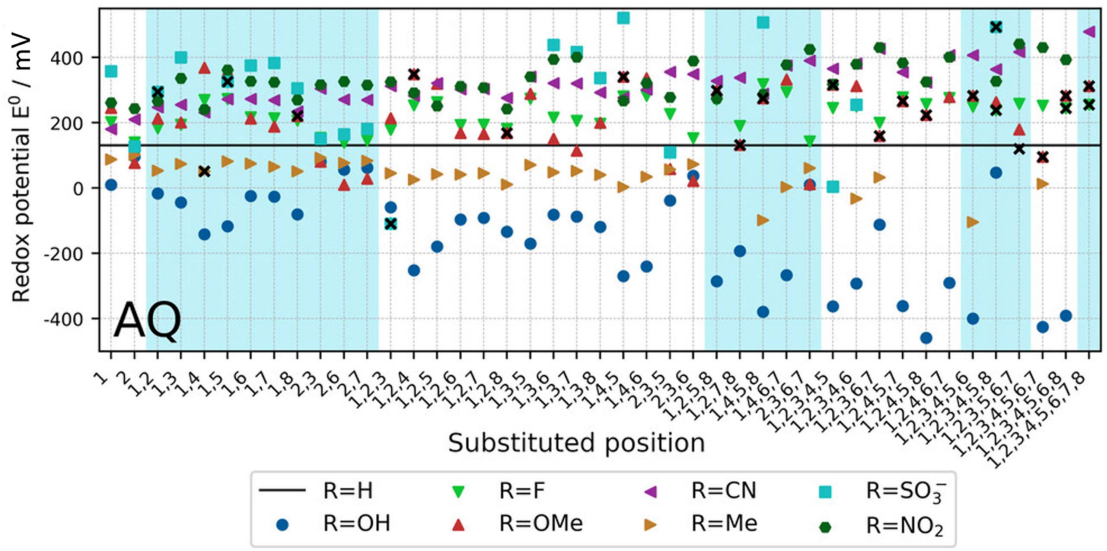

Figure 19. Calculated redox potentials of the AQ derivatives at the PBE-D3/aug-cc-pVDZ(PCM) level of theory (all values vs. SHE). The positions of the substituents are given on the *x*-axis. The black line indicates the redox potential of pristine AQ, the blue and white areas help to distinguish between the different numbers of substituents. The crossed-out data points represent molecules with a dihedral distortion within the ring system of more than 22°, which are considered to have a low stability. Taken from[150] and modified, John Wiley & Sons. [© 2020 The Authors. Published by Wiley-VCH GmbH].

LUMO energy. Moreover, a correlation was found between high solubility and most negative and positive redox potentials: molecules with low redox potentials are more soluble [138]. A correlation between electron affinity and redox potentials in quinone based systems was also confirmed at PBE0/6-31+G(d,p) level of theory for naphthaquinones and anthraquinones [148]. Furthermore, a strong influence of hydroxyl substitution on the redox potential was described. Modification of the molecular structures to improve the chemical and electrochemical properties of various quinone cores such as benzene, naphthalene, and anthracene opened up a large class of active materials and a large area for theoretical screening [149–152]. The latter was carried out with DFT using PBE and B3LYP density functionals. Variation of the quinone core structures and side groups in theoretical studies provide redox potential changes for different systems with quinone groups in the range of −0.8 up to 1.6 V vs. SHE. The effect of electron-withdrawing and electron-donating groups is most important in influencing the redox potential during structural changes. The screening studies demonstrate, as expected, that electron donating groups such as –OMe, –SH, –OH, $–NH_2$ decrease the redox potential, while electron withdrawing groups such as –F, –CN, $–NO_2$, –COOH increase it. Due to the π-conjugation of the aromatic core structure, the mesomeric effect has a much greater influence than the inductive effect. Furthermore, a non-trivial effect of the –OH groups was confirmed in the screening study (figure 19) by Schwan *et al* [150]. This study found that intramolecular hydrogen bonds between the quinone group and the hydroxyl group lead to an anomalous increase in the redox potential [150].

Modification of anthraquinones with amino groups changes the redox properties, the electrochemical reactions become reversible by oxidation due to electron donating effect of amino groups. The four-electron oxidation of tetra-aminoantraquinone was experimentally demonstrated in the work of Pahlevaninezhad and calculations were provided at B3LYP(PCM, DMSO)/6-31+G(d,p) level of theory [134].

In addition to the redox potential and solubility, it is important to estimate the stability of the screened molecules. This was done for quinone-based materials with the substituents of carboxylic, phosphonic and sulfonic acid. For these, the specific side reactions of Michael addition and the formation of gem-diols were taken into account. To perform the more than 1000 000 calculations, Tabor *et al* combined their DFT study with the application of semi-empirical methods [137]. The theoretical results demonstrate good agreement with experimental observations. The data analysis suggests that redox potentials themselves can serve as stability criteria, since molecules with too high redox potentials are typically unstable. The instability of systems with redox potentials higher than 1.0 V occurs due to Michael addition reactions [137].

Another approach to estimate the stability of the compounds was introduced by Schwan *et al* [150]. They developed and discussed structural descriptors for quinone-based systems based on the change in dihedral angles of the planar ring structures. The deformation of the planar structure was used to estimate the

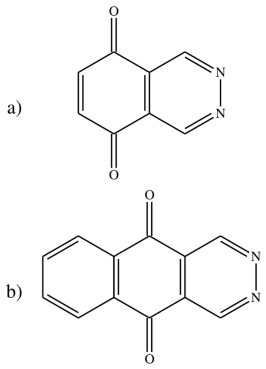

Figure 20. (a) Phthalazine. (b) 2,3-diaza-anthraquinone.

stability. Large changes in dihedral angle were associated with instability [150]. The basis of this approach goes back to the work of Zhigalko *et al*, who found that non-planar geometries for benzene, naphthalene and anthracene are only possible up to some limiting dihedral angles [153]. The search for stability descriptors is an important challenge for screening applications and may be beneficial for the development of RFBs active materials.

In other screening research, the solubility of 1,400 molecules was studied by the analysis of hydration energies using the Hartree–Fock method for the structural calculations in combination with MM constant density calculations DFT-GAFF and a simple point charge (SPC/E) solvent model for water. Higher hydration energies were found for quinones with the functional groups –CHO, –$COOCH_3$, –COOH, –PO_3H_2 and –SO_3H [154].

Waas *et al* showed that the commonly used DFT/B3LYP approach to calculate the geometric structures and redox potentials of quinones predicts the same trends as obtained at the CCSD(T) and perturbation theory levels of theory [155]. The accuracy of the MP2 method is comparable to that of DFT/B3LYP but has slower convergence of results with basis set size. MP2 overestimates the Gibbs free reaction energy by ∼20% compared to CCSD(T) and B3LYP.

Apart from the method, the modeling of the solvent environment is also an important aspect. Kim *et al* showed that by employing the solvent model PCM, the redox potentials of anthraquinone derivatives with ether groups at low pH value have a large mean absolute deviation of 194 mV compared to values from the corresponding experiments. They showed that the application of the QM/MM approach with an explicit description of the solvent effect leads to reliable results and corrects the errors of the implicit models [140]. Despite possible errors, implicit solvent models such as SMD and COSMO are the most common way to include environmental effects into quantum chemical calculations and in most cases provide satisfactory results compared to explicit solvent models [140, 156, 157].

Screening studies of quinone derivatives were already successfully carried out to investigate trends in the redox potentials and solubility. Challenges remain in the screening of stability against side reactions or synthetic availability. The former can be partially solved by applying semi-empirical methods or by developing descriptors [30].

Naphthaquinones and antraquinones can be substituted with heteroatoms in the aromatic core. An example studied in the context of RFBs are phthalazine, aza-anthraquinones and their derivatives. The molecules have positive potential shifts in comparison to unsubstituted quinones due to a stronger electronegativity of the nitrogen compared to carbon [141, 158]. Theoretical calculations of the compounds at PBE-D3(BJ) (PCM, water)/aug-cc-pVDZ level of theory for phthalazine (figure 20(a)) and at B86-D3(BJ) (PCM, water)/aug-cc-pVDZ for 2,3-diaza-anthraquinone (figure 20(b)) result in very good agreement with experimental redox potentials in acidic medium. Nevertheless, there are significant deviations for potentials in basic medium [141]. A possible reason for this difference could be that the redox reaction follows a different mechanism in basic medium.

The HOMOs and LUMOs of the 2,3-diaza-anthraquinone are given in figure 21. At the electronic level of theory, the reaction mechanism is the same as for anthraquinones. The LUMO of the molecule becomes the HOMO and stabilizes the central ring of the aromatic structure after a two-electron and two-proton transfer in acidic medium. The difference to the anthraquinone without heteroatoms is the small anti-symmetry of the electron density distribution with a shift towards the more electronegative nitrogen atoms. This is clearly visible for the HOMO of the oxidized form.

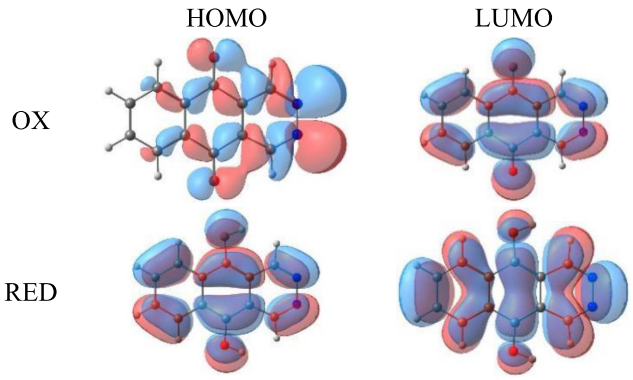

Figure 21. HOMO and LUMO of 2,3-diaza-anthraquinone at the PBE-D3BJ(PCM, water)/aug-cc-pVDZ level of theory (Isodensity value = 0.0145). Color coding: H (white), C (grey), O (red), N (blue).

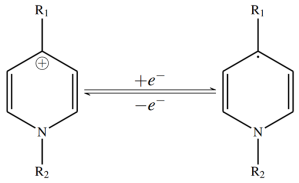

Figure 22. One-electron reduction of pyridinium cation-based anolyte core structure with formation of the pyridyl radical.

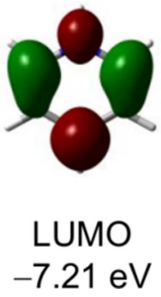

Figure 23. LUMO of the pyridyl moiety with $R_1 = R_2 = H$ calculated at the B3LYP/6-311G(d,p) level of theory. Reprinted with permission from [164]. Copyright (2020) American Chemical Society. Color coding: H (white), C (grey), N (blue).

3.5. Nitrogen-containing molecules

Nitrogen-containing molecules are a large class of promising redox active materials for RFBs. This class overlaps with the classes of radicals and substituted quinones and represents such molecules modified with nitrogen-containing groups, and with nitrogen-containing core structures.

3.5.1. Pyridinium-based systems

Pyridine-based cations form an important class of anolyte-active materials [159]. These cations react to radicals in a one-electron reduction reaction, see figure 22. The electron is transferred to the LUMO (figure 23) and delocalized over the heterocyclic core. For the theoretical description of these compounds at the DFT level of theory, the B1B95 density functional was recommended for one-electron redox reactions. The calculated redox potential differs from the experimental results by less than 0.02 V [160]. Most of the known materials in this group are dipyridyl systems with a viologen core structure in which two-electron reductions occur. Here, the cation radical is formed in a one-electron reduction and can be further reduced to a neutral molecule (figure 24). The first and second reduction potentials for methyl viologen in aqueous medium are $E_0 = -0.45$ V and $E_0 = -0.76$ V vs. SHE (R_2 = Me) [161, 162]. Korshunov *et al* experimentally obtained 9% variation in the redox potential for the viologen-based molecules and their structural design using host-guest type supramolecular complexes [163].

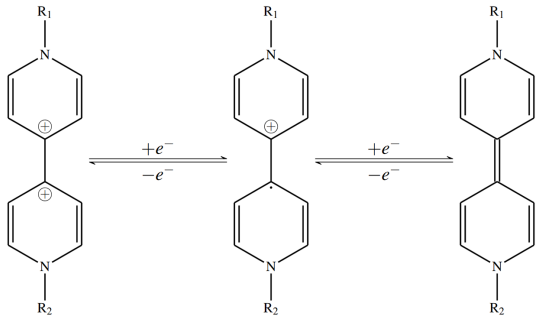

Figure 24. Two-electron reduction of the viologen dication (containing two pyridyl cores). The first reduction leads to a viologen cation radical and the second to the formation of an additional double bond.

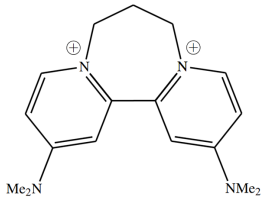

Figure 25. Bispyridinylidene dication.

The substituents R_1 and R_2 affect the redox potentials. The corresponding HOMO-LUMO energies were experimentally and theoretically studied. Theoretical calculations were performed at the M06-2X (SMD, water)/6-31+g(d,p) level of theory and confirm the electronic donor and acceptor effects for the viologen-containing systems as well as for other systems discussed. Smaller HOMO-LUMO splitting leads to higher reduction potentials [165, 166].

Another cationic bispyridinylidene anolyte (figure 25) with a high specific capacity and a reduction potential of −1.00 V vs. SHE was experimentally studied by Alkhayri and Dyker [167]. In addition, uncharged pyridine derivatives were reported as compounds with low redox potentials in the range of −2.03 to −0.28 V vs. SHE [168]. A bipolar system in combination with a TEMPO structural core was also synthesized and investigated. The compound combines the advantages of viologen and TEMPO. It has an energy density of over 16 Wh $l^{-1}$and a high retention rate [94]. The electronic structure calculated at the DFT-B3LYP/6-31G* level of theory with an implicit solvation model (SMD) shows that the LUMO of the molecule is almost identical to the corresponding orbital of TEMPO and the HOMO contains a larger contribution of the viologen molecular fragment [94].

Kannappan *et al* studied the redox chemistry and structure of viologen derivatives that contain two linked viologen structural fragments by experiment and theoretical calculations at DFT-B3LYP and MP2 level of theories. The results of x-ray structural information and measured electronic structure properties demonstrate agreement with theoretical calculations. The calculations performed allowed to obtain structural information on the singlet- and triplet-state π-dimerized bis-viologen species [169].

3.5.2. The succinimid structural core

The next nitrogen-containing anolyte material discussed is *N*-Methylphthalimide, which is reduced to an anion radical [$E_0 = -1.06$ V and −1.34 V vs. SHE [approximated by Ag^+/Ag (0.1 M $AgNO_3$ ACN) in acetonitrile reference electrode potential), ionic liquid] [170]. The reduction is achieved by an one-electron transfer with formation of an anion radical, see figure 26. *N*-Methylphthalimide was used as the catholyte in the combination with a TEMPO-based molecule. Stable charging and discharging with high coulombic efficiency (90%) was achieved for the first few cycles [171].

The system was found to be a potentially interesting redox active material even with additional quinone groups. This is based on the DFT calculations at PBE-D3/aug-cc-pVDZ level of theory in water (described with the PCM), which predicted a high redox potential of 1.14 V vs. SHE for the quinone structure with the *N*-Methylphthalimide core [denoted as dihydroxyphthalazine(sumi) (DHP(sumi))], see figure 27 (R = H), in a screening study with 42 molecules [158]. At the same time, the stability based on the deformation of the cyclic planar system was estimated to be low for some substituted DHP derivatives due to high dihedral angles. However, synthetic availability cannot simply be verified by the structural deformation analysis. The

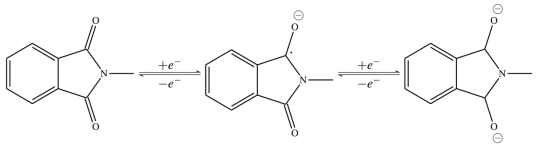

Figure 26. Two-step reduction of *N*-Methylphthalimide to the corresponding dianion.

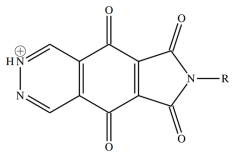

Figure 27. Theoretically predicted structure of DHP(sumi) as a promising redox-active material (oxidized form).

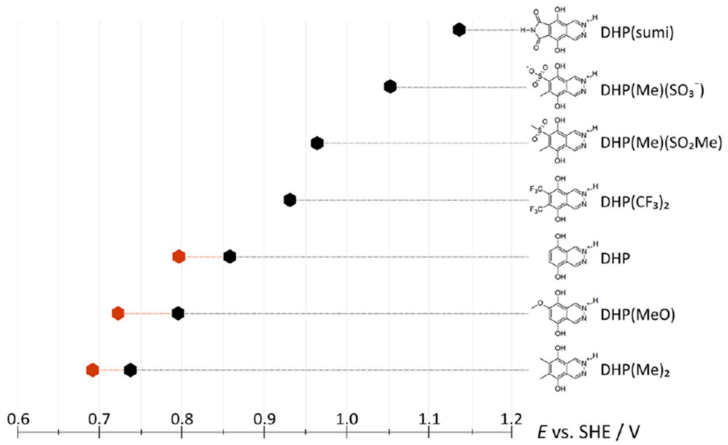

Figure 28. Overview of selected calculated E_{calc} (black symbols) and experimental values (red symbols) for different DHP substitution patterns (pH = 0). Reprinted with permission from [158]. Copyright (2020) American Chemical Society.

same redox activity as for the quinones of DHP(sumi) has been considered by Hoffman *et al* [158]. However, reactivity at the succinimide moiety is also possible and can be considered as a possible side reaction. The results of the screening efforts are presented in figure 28.

3.5.3. Phenazine-based structures

The next major and very promising class of nitrogen-containing heterocyclic systems are the phenazine-based redox active materials [172–176]. The reduction reaction of phenazine in aprotic medium is shown in figure 29. During the reduction of the phenazine in aqueous media, the nitrogen atom is protonated [177]. There is a two-electron transfer to the LUMO and destruction of the aromatic electronic structure of the central ring. As a result, the molecule in the reduced form is no longer flat, and the electronic structure at the N-atoms acquires an electronic configuration with sp^3 hybrid orbitals. These structural changes result in out of plane deformation and a loss of the π-conjugation throughout the molecule. However, a recent study reports a planar structure of a disubstituted reduced form of the phenazine structural core [178]. The redox potential of the reaction is −0.94 V in ACN [179] and −0.99 V in DME [180] vs. SHE. The main challenge with phenazine-based systems is usually the low solubility, while the system has good electrochemical stability [30]. The solubility issue can be addressed by molecular modification with additional functional groups such as sulphonic (–SO_3H) or carboxylic acid (–COOH) [91, 176].

A detailed theoretical study of the solvation issue and redox potentials of various phenazine derivatives was presented by Zhang at B3LYP(COSMO, water)/DNP level of theory [181]. Solvation energies and redox potentials for reactions with two-electron and two-proton transfer were calculated. Correlation of LUMO energies and redox potentials shows that the redox potential decreases mostly linearly with increasing LUMO energy. The calculated redox potentials are in very good agreement with the experimental results. The correlation of the solvation energies with experimental solubility was also determined.

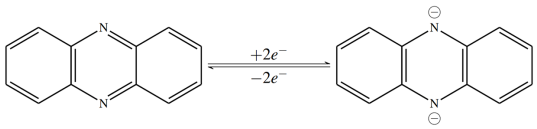

Figure 29. Two-electron reduction of phenazine without protonation at the two nitrogen atoms. The reduction leads to destruction of the π-conjugation in the central ring and deformation of the molecule.

Screening studies of the redox potentials of phenazine derivatives were presented by de la Cruz *et al* [182]. The electron withdrawing effect was confirmed and is much stronger than for anthraquinones (potential change 1.3 V compared to 0.5 V for anthraquinones). Reorganization energies and root mean square deviations were used for comparison of stability. A more negative shift of the redox potential was discovered for electron donating groups in position R_2 compared to position R_1. As with quinones, the high stability of the molecules in electrochemical reactions opens up great application prospects. Tuning of the redox properties by modification and molecular design can further improve this redox active material. In the fully reduced and oxidized forms, the molecules are closed-shell electronic systems that can be efficiently explored by DFT-based methods. This was already done, for example, in a screening study at the B3LYP(SMD, water)/6-31+G(d) level of theory presented by Assary *et al* [183]. In any case, in the theoretical study of phenazine derivatives, the correct protonation of the reduced and oxidized forms must be considered, as this affects the thermodynamic energy and influences the prediction of the redox potentials. Therefore, the correct inclusion of solvation effects with implicit solvent models and the consideration of different possible protonation types is necessary for reliable and correct results.

The combination of nitrogen-containing heterocyclic systems with quinones was investigated as potential electrolytes for symmetrical RFBs in the theoretical screening research of Fornary *et al* at the DFT-B3LYP/6-311G(d,p) (PCM, water) level of theory [184]. In this study, the dependency of the redox potential on molecular structures and heteroatom positions and solubility was studied. Structure-property relationships were predicted and analyzed for potentially interesting phenazine-based redox active materials. The study considered different substitutions at the aromatic system with heteroatoms containing several redox units in one molecule. Interactions at the electronic level between different redox units and intramolecular hydrogen bonding were identified as factors influencing the redox potential. The solubility differences between the compounds studied can be up to four orders of magnitude, and the redox potentials are in the range from −0.5 V for reduction up to 1.4 V for oxidation (SHE).

The redox potential shift due to the modification of the phenazine structure with electron donating and electron withdrawing groups was also confirmed for phenazine based structures at LC-wPBE/6-311+G(d,p), B3LYP/6-31G+(d) (PCM, water) and at PW91(COSMO, water)/DNP levels of theory [185–187]. The protonation effect on the redox potential of single functionalised phenazine derivatives is not large, with changes in the range of 200 mV between the amino and carboxylic groups. This indicates that the destruction of aromaticity during the reaction reduces the influence of the mesomeric effect on the redox potential shift due to the loss of conjugation in the reduced form. Variation of the phenazine structural core with additional pyridine rings could change the redox potential more significantly by a stronger influence of the electronic structure on the redox centers. The addition of extra pyridine rings to the phenazine structure decreases the redox potential by 0.2 V [187].

ML methods using four regression models were applied to DFT calculated results of redox potentials by Ghule *et al* [40]. A small data set with 151 phenazine derivatives containing 20 unique functional groups was used to train the models based on automatic relevance determination regression, Gaussian process regression, kernel ridge regression and support vector regression. The trained models achieved high accuracy with a coefficient of determination $R^2 > 0.74$ compared to DFT reference calculations for all used models.

3.5.4. Azobenzene

A non-aqueous high capacity RFB based on azobenzene (AB) as anolyte was reported [35, 188]. A two-electron reduction to the corresponding anion occurs during the reaction, see figure 30. This leads to a stronger delocalization of the electron density (figure 31) and electrostatic stretching of the central N–N bond. Azobenzene has a redox potential of −1.22 V vs. SHE in ACN [188, 189]. Unfortunately, azobenzene is not stable in protic systems and shows decomposition tendencies such as dimerization reactions or disproportionation [36].

Zu *et al* studied the solubility of different azobenzene derivatives at the DFT level of theory. By modifying the basic structure with strong hydrophilic groups, several derivatives such as 4-amino-1,1′-azobenzene-3,4′-disulphonic acid monosodium salts represent promising anolytes with

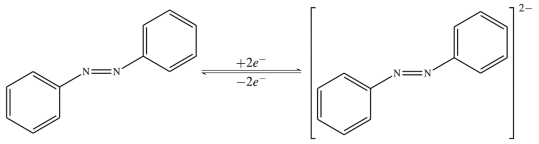

Figure 30. Two-electron reduction reaction of azobenzene to azobenzenium dianion in an aprotic environment.

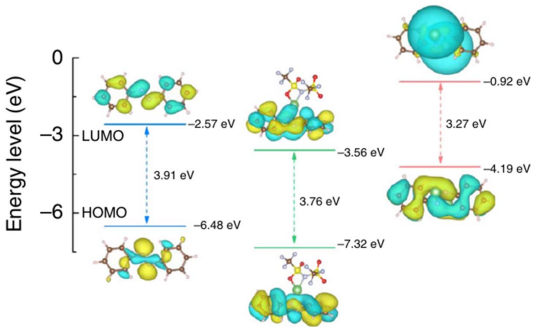

Figure 31. Optimised structure and calculated energy levels of AB, AB-LiTFSI, and Li_2AB obtained from DFT (B3LYP/6–311G++(d,p)) calculations. Color coding: H (white), C (brown), N (grey), O (red), S (yellow), Li (green), F (grey). Reproduced from [188]. CC BY 4.0.

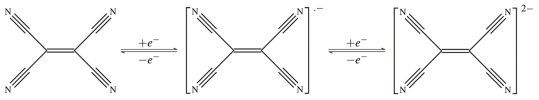

Figure 32. Two-step reduction to tetracyanoethylenium dianion.

high-performance for aqueous systems [35]. The geometric structure of azobenzene was studied in detail at CC2 and MP2/cc-pVTZ levels of theory and compared to DFT (BP86, B3LYP) and to experimental results by Fliegl *et al* [190]. DFT provides reliable results for structural parameters and vibrational frequencies compared to experimental values, but not for electronic structure and excitation energies. Vibrational frequency spectra calculated by MP2 show a tendency to blue-shift, while DFT frequencies are usually slightly red-shifted. In conclusion, wave function-based methods are recommended by the authors as the methods of choice for investigating substituent effects on the structure and optical properties of azobenzenes [190].

3.5.5. Tetracyanoethylene

Molecules with delocalized electrons in combination with cyano-groups show promising redox activity. For example, Wang *et al* studied the redox activity of tetracyanoethylene (TCNE) (see figure 32) as an anolyte [191]. A reduction reaction was observed with two peaks at 0.49 and −0.54 V vs. SHE in ACN (recalculated for $Ag/AgNO_3$ (0.01 M, ACN)).

The reduction reaction involves a two-electron transfer in which the LUMO of the TCNE molecule becomes occupied and becomes the HOMO of the corresponding anion.

Theoretical calculations showed that the molecular orbital energies increase from the neutral form to the fully anionic form, see figure 33. The C=C bonding contributions in the HOMO and the C=C antibonding contributions in the LUMO indicate the nodal plane of the wave functions perpendicular to the bond. There is also a strong delocalisation in the LUMO for the fully reduced $TCNE^{2-}$ compared to the single charged molecule.

3.5.6. Summary of theoretical studies of nitrogen-containing molecules for RFB

Nitrogen-containing molecules are probably the largest class of promising redox active materials for organic RFBs [37]. The systems have a wide range of applications and therefore many theoretical studies were performed. Calculations of the electrochemical properties provide useful information on the structure, design, and the applicability of different theoretical methods. In most cases, DFT calculations give at least qualitatively correct results. The DFT calculations are successfully used to predict various experimental

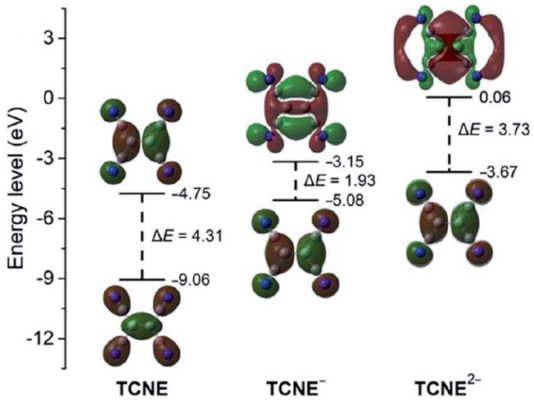

Figure 33. Molecular orbitals (HOMO and LUMO) of the neutral and reduced states of TCNE calculated at DFT level of theory. Reproduced from [191] with permission from the Royal Society of Chemistry. Color coding: C (grey), N (blue).

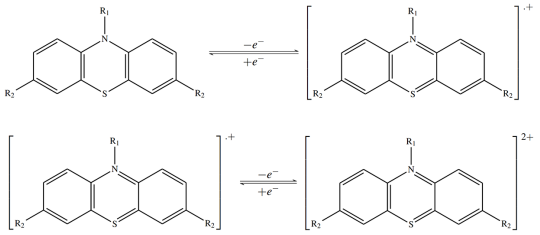

Figure 34. The core structure of phenothiazine and its oxidation in a two-step reaction to the aromatic phenothiazinium dication in an aprotic environment.

trends and in screening research. Not all systems in this class were sufficiently theoretically studied. This leaves room for screening studies of solvation energies and redox potentials as well as the calculation of explicit electrochemical reactions and the exploration of degradation mechanisms with theoretical methods. However, the quantum chemical description of ion-radical systems or intermediates such as the azo radical anion $ArNNAr^{-}$ in reduction reactions needs to be carefully analyzed at the DFT level of theory. The DFT calculations may contain localization-delocalization errors and spin contamination. Such systems may exhibit multi-reference character and require multi-reference approaches for accurate description.

The combination of nitrogen-containing fragments with other redox active moieties such as quinones leads to a variety of possible redox reaction products. These complex molecules with multiple redox active centers require careful analysis as different redox reaction pathways may occur at different reaction centers. In this case, the stability and reaction mechanism should be considered for different possible reaction products.

In addition, the interaction of redox-active molecules with their environment is not correctly described by implicit solvent models when reactions with the solvent occur. For example, the protonation of nitrogen atoms and hydrogen bonding have a strong influence on the redox potential and electrochemical properties. Therefore, different reaction mechanisms must be considered, including different degrees of protonation. In addition, the correctness of the model systems should be carefully analyzed with chemical intuition before the theoretical calculations are performed.

3.6. Sulphur-nitrogen-containing heterocyclic molecules

3.6.1. Phenothiazine-based structures

Other classes of redox-active molecules with a heterocyclic core are represented by molecules in which the nitrogen atom in the basic nitrogen-containing compound is replaced by sulphur or oxygen. A typical example is the class of phenothiazine-based structures that can be used as catholytes in RFBs, see figure 34 [36]. These are phenazine-like structures in which one nitrogen atom is replaced by a sulphur atom. The redox potentials of the two-electron oxidations (figure 35) (with $R_1 = –CH_3$, $R_2 = H$) are 0.95 V and 1.55 V vs. SHE in ACN [192]. Figure 39 shows the change in the HOMOs during the electron transitions. After the single-electron oxidation, the HOMO of phenothiazine becomes more localized in the aromatic core. After the second oxidation, an energetically lower orbital becomes the new HOMO. This leads to aromatization of the central ring and high stability of the cation.

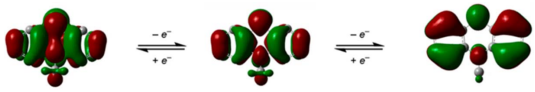

Figure 35. Visualization of the HOMO and SOMO *N*-methylphenothiazine calculated at the B3LYP/6-31G(d) level of theory. Reprinted with permission from [193]. Copyright (2021) American Chemical Society.

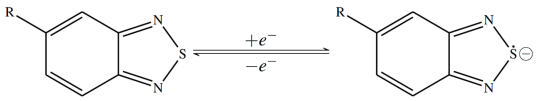

Figure 36. One-electron reduction of 2,1,3-benzothiadiazole to the anion radical of 2,1,3-benzothiadiazole in an aprotic environment.

Redox potential calculations of phenothiazine and *N*-methylphenothiazine in acetonitrile (PCM) at the DFT (B3LYP, B3PW91) and Hartree–Fock levels of theory were performed by Rawashdeh with Pople basis sets. While the Hartree–Fock method correctly describes the geometric structure, the redox potentials are strongly underestimated. The best agreement with experimental results (100 mV deviation) was obtained using the B3PW91/6-311+G* method [194].

The influence of electron-donating and withdrawing groups on the orbital energies of these molecules was studied in several investigations at DFT/B3LYP-D3/TZ2P, TD-DFT:M052x/6-31G(d), B3LYP/6-311G(d,p) levels of theory. The results follow the trend of experimental redox potential measurements. A decrease in the HOMO energy due to electron withdrawing substituents leads to higher redox potentials of the phenothiazine derivatives. Electron donating groups decrease the redox potential [192, 195–199]. Redox potential variations of 0.84 V–1.08 V vs. SHE in the first oxidation step and 1.45 V–1.66 V vs. SHE in the second oxidation step were reported for methyl groups and chlorine atoms at R_2 position [192]. Thus, phenothiazine and phenazine exhibit the same tendencies.

3.6.2. Benzothiadiazole based molecules

Another sulphur-containing structure of interest for RFBs is 2,1,3-benzothiadiazole (BzNSN) [87]. The molecule transforms into an anion-radical on reduction with one electron and has a similar geometric structure as the benzo-1,2,3-dithiazolyle radical discussed in section 3.3.4 (figure 36). BzNSN has a low reduction potential of −1.05 V vs. SHE in ACN and is relatively stable in non-aqueous solvents [200]. Further modification of the basic structure with the replacement of the sulphur atom by nitrogen was reported in experimental research as a new promising class of low potential anolytes [201].

The electronic properties of BzNSN derivatives have been considered in several studies at the DFT level of theory. The influence of electron donating and withdrawing groups on the redox potentials was demonstrated at the B3LYP/cc-pVDZ level of theory. Substituents containing heteroatoms with higher electron affinity than N increase the oxidation potential and decrease the HOMO energy compared to substituents containing electron-rich atoms such as Se [202]. Moreover, the shift of optical absorption and emission for substituted molecules due to electrochemical reduction and oxidation has been confirmed by TDDFT calculations at the B3LYP/cc-pVDZ, B3LYP/def2-TZVP and M08-HX/6-311++G(d,p) levels of theory [202–204]. Despite the deviations in the predicted values, the theoretical results describe the tendencies of substitution effects on the redox potential qualitatively correctly in comparison to experimental results.

The adsorption of BzNSN on a graphene electrode was modeled at the PBE-D3/pw level of theory by Howard *et al.* They demonstrate a strong interaction of the molecules with surface defects [205]. These results predict passivation of reactive defects on graphene electrodes in battery technologies.

3.6.3. Summary on theoretical studies of sulfur-nitrogen-containing molecules for RFB

Sulphur atoms as heteroatoms in aromatic molecules shift the electronic density compared to nitrogen-only systems. This usually causes a shift in the redox potentials, with values decreasing when sulphur is introduced. This was confirmed in a theoretical screening study by replacing heteroatoms in cyclic structures [206]. A detailed theoretical consideration of the electronic structure and redox activity in the context of RFBs is not yet available. An exception represents the group of the phenothiazine-based structures.

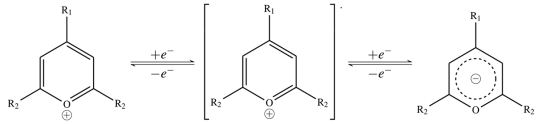

Figure 37. One- and two-electron reduction of an isolated pyrylium ion to the radical in the first step and to the pyrylate anion in the second step in an aprotic environment.

3.7. Pyrylium ions-containing systems

Antoni reported about the synthesis of a potentially useful compound containing pyrylium ions (figure 37) that could be used in RFBs [207]. The molecular structure is very similar to pyridine-based active materials, with nitrogen replaced by oxygen. The positive charge in the oxygen is delocalized across the aromatic system, but there is also a tendency to concentrate on neighboring carbon atoms, leading to a cationic character [208]. The redox reaction of isolated pyrylium and thiopyrylium structures was described by Saeva. It can be understood as a one-electron process with reduction to a radical or a two electron process with reduction to a corresponding anion with charge localization at the oxygen atom (figure 37) [209]. Derivatives such as pyrylenes can have high reduction potentials ($E^0 = 0.77$ V vs. SHE) and be strong oxidants [207]. However, the stability of such organic ions is questionable as various degradation reactions such as dimerization of the radical form can take place [210]. The stabilization of pyrylium systems by functionalization with carbenes was discussed in this context. But here the reduction mechanism becomes more complicated because of electronic conjugation [207].

The coordination of counter ions such as halogen anions to the pyrylium structure was investigated at MP2/6-311++G** and B3LYP/6-311++G(d,p)(6d,10f) levels of theory in DMSO and benzene (PCM) by Milov *et al* [211]. The cationic nature of the pyrylium was confirmed by the coordination of the counterions to the carbon atoms. They also demonstrated the importance of counterions in stabilizing the pyrylium structure due to the electron density distribution and a covalent bond formed between the counter ion and pyrylium. DFT and MP2 methods provide similar structural information and zero-point frequencies for the pyrylium ion [211]. Optical spectra (UV–Vis) of pyrylium based structures calculated by TDDFT at the B3LYP/6-31G(d) level of theory are in only approximate qualitative agreement with experimentally measured spectra [212]. A detailed theoretical description of pyrylium-water complexes at the B3LYP/6-31+G(d,p) level of theory and analysis of molecular orbitals was carried out by Parreira and Galembeck [213]. No significant change in the pyrylium structure was found as a result of coordination to water. This is due to the weak hydrogen bonding of the pyrylium C–H group with the water molecules. The coordination of the water molecules was confirmed to take place on carbon atoms at position 2 and 6 of the pyrylium ring. Orbital analysis shows *s*- and *p*-character of the bonding orbitals within the coordination.

Pyrylium-based structures have the potential to be used as active materials for RFBs, although studies are so far rare. Oxygen atoms as heteroatoms in aromatic molecules shift the electronic density to higher redox potentials. Detailed theoretical consideration of the electronic structure and redox activity of these molecules in the context of RFBs active materials are not investigated or presented.

3.8. Organometallic complexes

Another interesting class of active materials, both from a practical and theoretical point of view, is the combination of organic materials with metal atoms. The combination of fine-tuned organic materials with stable properties and metal ions also represents a RFB class of redox active materials. Here we give only a brief overview of this very large class of active materials and discuss some representative computational investigations.

Organometallic compounds utilize metal ions in non-aqueous systems with fast kinetics. A classic example of organometallic active materials is metallocene complexes (figure 38). The redox reaction in these compounds is accompanied by a change in the oxidation state of the central ions. Battery systems with these active materials usually contain charge carriers such as Li ions [214]. HOMOs and LUMOs of ferrocene (Fc) in the oxidation reaction are presented as an example in figure 39. The qualitative change of the d_{yz} orbital due to the superposition with p orbitals is clearly visible.

Properties can be varied by additional functionalization of the cyclopentadienyl rings of the metallocene with one or a few organic substituents. The same molecular design by substitution is possible as in the case of purely organic active material modifications (R groups in figure 38). The redox potentials of one-electron reactions M^+/M^0 can thus be varied over a wide range from −1.23 V to 0.79 V vs SHE [216].

In addition to metallocenes, a large number of other complexes were used as active materials in RFBs. Typical examples are various complexes of bipyridine (bpy) derivatives and metal acetylacetonate derivatives

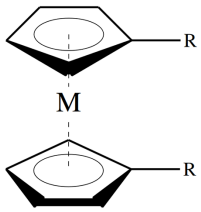

Figure 38. General structure of a metallocene complex where M = V, Cr, Mn, Fe, Co, Ni, Ru, Rh and R = any organic functional groups.

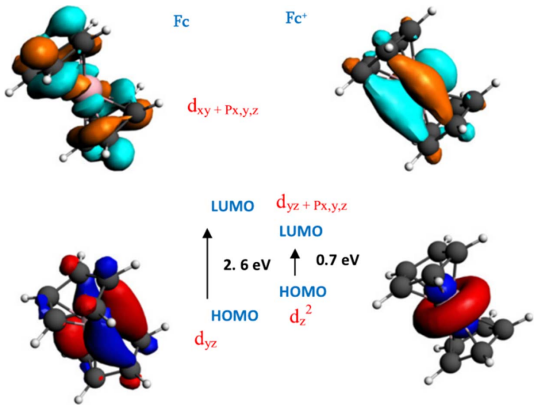

Figure 39. Ferrocene molecular orbitals in a one-electron oxidation reaction with their energetic gaps in the gas phase (DFT-PBE) [215]. Color coding: H (white), C (grey), Fe (pink); red/blue—HOMOs, orange/cyan—LUMOs. Reproduced from [215]. © 2015 The Royal Swedish Academy of Sciences. All rights reserved.

[217]. Some complexes with a heavy atomic core such as U or Ru were also explored for use as electrolytes. Several complexes such as $[Ru(bpy)_3(BF_4)_2]$ have high cell voltages of up to 2.6 V and thus great potential for future application [217].

The theoretical calculations of systems with bipyridine ligands and different metallic cores require more accurate approaches than standard DFT due to the breakdown of hybrid and double hybrid functionals in the electronic structure calculations. DFT calculations lead to the prediction of an incorrect spin-state. Therefore, even the energetics of the redox reactions cannot be reliable estimated. The theoretical prediction of other measurable parameters of the molecules at the DFT level of theory is also questionable. Thus, these calculations require more powerful electronic structure theory methods. The DFT failure was investigated e.g. by Drosou *et al* [218] and Milko and Iron [219] at CASSCF/NEVPT2/def2-TZVPP level of theory and described as being caused by the multi-reference nature of the underlying structures. However, several of the GGA functionals considered such as τ-HCTH and HCTH can also describe the electronic states with relatively small errors [219]. The problem of the identification of coordination complexes with multi-referent ground states at the DFT level of theory was also discussed in the work of Shee *et al* [220]. The successful application of auxiliary field quantum Monte–Carlo methods with cc-pVXZ-DKH basis sets was demonstrated with high accuracy for the calculation of redox potentials of metallocenes with multi-configurational wave functions. This methodological approach has a scaling factor of $O(N^4)$ with Gaussian basis sets, and looks very promising for challenges involving the description of multi-referent character, symmetry breaking states and similar problems [80].

The theoretical exploration of other organometallic systems with cores such as Cr, V, Mn, Fe, Ru showed that for screening of various parameters such as redox potentials and solubilities, DFT (PCM, acetonitrile)-B3LYP/6-31+G(d) can provide reliable results. In the study by Kucharyson, the calculations were performed for ferrocene and acetylacetonates-based complexes [221]. A correlation was found between the electron density on the metal ions and electrochemical stability. This is a potentially interesting descriptor of stability. The orbital energies of ferrocene in one-electron oxidation reactions in vacuum were studied at DFT-PBE level of theory. A shift of the HOMO-LUMO gap to lower energies after oxidation and conversely a shift to higher energies upon reduction back to the neutral state were identified [215]. The previously discussed change in the orbital overlap due to one-electron oxidation is an interesting phenomenon, which may indicate changes in chemical bonding in the underlying system (see figure 39).

Theoretical investigations of organometallic complexes are also important for understanding the complex mechanisms of electrochemical reactions of the material class. In this context, the stability of lithium complexes with 1,2,3,4-tetrahydro-6,7-dimethoxy-1,1,4,4-tetramethylnaphthalene (TDT) in different oxidation states was successfully explained at the B3LYP/6-31+G(d) level of theory with the SMD solvent model by Carino *et al.* Using a combined DFT and *in situ* spectroscopic approach, the coordination of neutral TDT molecules with lithium ions was determined and confirmed [222].

In summary, organometallic complexes show possible advantages of the organic system compared to metal-based electrolytes in terms of structural flexibility, and advantages of the metal ions in terms of high oxidation state stability. Moreover, complexes can be important objects of investigation as intermediates in mechanisms of redox reactions in battery systems with metal ion charge carriers. The theoretical description of organometallics in screening studies and the understanding of reactions and degradation mechanisms can be more difficult due to the complex electronic structure, which can have a multi-reference character already for ground states. Due to the size of the systems and the complexity of the electronic structure, systematic methodological approaches for screening studies are an important challenge for quantum chemistry in the investigation of organometallic materials for RFBs.

4. Conclusions

The central components for energy storage in RFBs are the active materials in the anolyte and catholyte. Many different potentially redox-active organic materials from different classes are known today, such as radicals, quinones, nitrogen-containing molecules, heterocyclic systems with nitrogen, oxygen and sulphur, and organometallic complexes, all of which were considered in this review. The redox active materials were discussed from a theoretical point of view in terms of quantum chemical screening and investigations of the redox reactions. Theoretical studies are currently available for most of the classes of the redox active materials considered. However, some of these considerations are only superficial and not systematic enough. In-depth analysis of molecular and electronic structure, reaction mechanisms, or the correlation between electronic structure, redox properties and stability is often lacking. In addition, detailed descriptions, illustrations of the electronic structure and orbitals of molecules are sometimes missing.

Otherwise, theoretical screening is particularly important and useful. It can support experimental synthesis, as it is practically impossible to experimentally explore the large number of potential candidates for redox-active materials with highly variable structures. With the help of computational screening studies, a pre-selection can be made. Moreover, the influence of synthetic modifications such as substitutions of already well investigated basic structures on redox potentials, can be predicted at least qualitatively with standard quantum chemical approaches. DFT-based theoretical screening methods are now recognized as an efficient tool for helping to solve the practical problem of searching and designing redox-active materials for RFBs. The DFT based methods provide reasonable qualitative results for redox potentials in most cases and allow calculations with acceptable computational time. The main difficulty in using DFT lies in the choice of the density functional for the molecule class considered.

In general, DFT-based calculations of single-molecule reactions are employed using an implicit solvent model (COSMO, PCM, SMD), and the redox potential is the most important parameter for the primary screening studies. For most redox reactions involving closed-shell systems, DFT calculations with density functionals such as PBE and B3LYP provide reliable results regarding redox activity, solubility, and corresponding trends of structural modifications. Nevertheless, the analysis of such results should be carefully carried out, as the DFT method can fail for specific molecules and reactions [129, 218]. Theoretical results for radicals and systems with charge delocalization with potential electronic state degeneration may contain larger discrepancies compared to molecules with closed shell non-degenerated states. These molecules require careful analysis of the nature of the electron correlations. The prediction of different correlation types for products and reagents can lead to inconsistent description of the reaction energies at a chosen level of theory and requires careful selection of an appropriate quantum chemical method for all molecular forms in the reaction. Outside of the electronic structure description, errors in the predicted experimental parameters arise from the limitations of the solvent models used [140]. Additive errors in the absolute values of the redox potential can also arise from the chosen reference constants such as the absolute SHE potential. However, these deviations do not affect trends and are not linked to the correctness of quantum chemical calculations.

An important problem in the systematic screening is the prediction of the stability of potential organic redox active materials. This concerns molecules in all redox states. Due to the many types of degradation mechanisms, there is no universal descriptor of stability that is independent of the specific organic material. The search for both universal and powerful stability descriptors is probably one of the most important issues in computational screening methods. However, different stability descriptors have already been proposed.

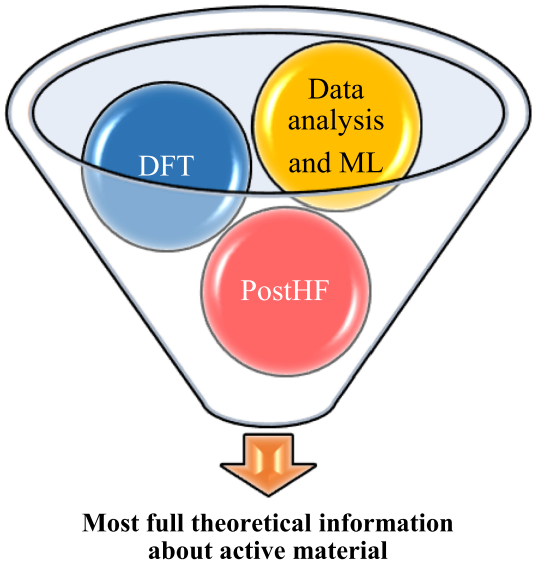

Figure 40. Combined approach for most fully theoretical analysis of active materials.

Examples of the different descriptors are reaction energies of possible side reactions [117], structure deformation energies based on dihedral angles [150], and electron density distributions at active centers. These represent useful descriptors for the selected basic structures but are not a universal approach for all compound classes [221]. The different system classes and structural fragments are most efficiently described by different descriptors.

Beyond DFT screening studies, there are two important directions for further theoretical consideration. The first is to generalize the screening data using statistical methods and ML tools [206] to further accelerate predictions for molecules of similar nature and their properties such as redox potential and solubility based on statistics. The integration of these new approaches is currently an innovative and developing research area. The second is the detailed theoretical investigation of potentially interesting candidates using more precise theoretical approaches such as wavefunction-based correlation methods, especially multireference methods. These will be used to verify the electronic ground state, to calculate reaction and degradation mechanisms, and to more accurately investigate experimentally measured parameters [130]. The detailed investigations provide information on reaction paths, kinetics and charge transfer in accordance with Marcus theory and transition state theory.

The future of the most efficient and thorough theoretical studies of active materials may therefore lie in combined hierarchical approaches (figure 40). First, the most interesting potential candidates are selected by calculations at lower levels of theories, such as DFT or yet more large-scale statistical analysis or semi empirical methods. Even at the basic DFT level, specific descriptors of molecular properties can be calculated to gain understanding of important trends: Orbital energies correlated with redox potentials, polarity indicating solubility, structural deformation energy as possible criteria of stability, etc. Second, a more detailed analysis using more expensive and in-depth theoretical methods such as CASSCF-based or quantum Monte-Carlo-based approaches will be used to confirm the electronic structure and clarify the values of interest as well as for a detailed analysis of reaction mechanisms or degradation mechanism. In addition, the synthetic availability will be assessed. In particular, the search for organic redox-active materials is a good example of applying methods from theoretical chemistry to solve practical technological problems.

Data availability statement

No new data were created or analysed in this study.

Acknowledgments

A Zaichenko, S Kunz, H A Wegner, J Janek and D Mollenhauer appreciate the financial support by the federal Ministry of Food and Agriculture (BMEL) within the project FOREST II (Projects: 2220HV053G, 2220HV053D and 2220HV053E). A J Achazi and D Mollenhauer appreciate the support from the German Research Foundation (SPP 2248, Project Number 441217366). A Zaichenko, S Kunz, H A Wegner, J Janek

and D Mollenhauer acknowledge the fruitful discussion and support from CMBlu Energy AG. J Janek acknowledges funding by the German Research Foundation (DFG) under Project ID 390874152 (POLiS Cluster of Excellence).

Conflict of interest

The authors declare no conflict of interest.

ORCID iDs

Aleksandr Zaichenko https://orcid.org/0000-0002-3486-2253
Andreas J Achazi https://orcid.org/0000-0002-3001-875X
Hermann A Wegner https://orcid.org/0000-0001-7260-6018
Jürgen Janek https://orcid.org/0000-0002-9221-4756
Doreen Mollenhauer https://orcid.org/0000-0003-0084-4599

References

[1] Abdmouleh Z, Alammari R A M and Gastli A 2015 Review of policies encouraging renewable energy integration & best practices *Renew. Sustain. Energy Rev.* **45** 249–62
[2] Żuk P and Żuk P 2022 National energy security or acceleration of transition? Energy policy after the war in Ukraine *Joule* **6** 709–12
[3] Juntunen J K and Martiskainen M 2021 Improving understanding of energy autonomy: a systematic review *Renew. Sustain. Energy Rev.* **141** 110797
[4] Alstone P, Gershenson D and Kammen D M 2015 Decentralized energy systems for clean electricity access *Nat. Clim. Change* **5** 305–14
[5] Cappers P, MacDonald J, Goldman C and Ma O 2013 An assessment of market and policy barriers for demand response providing ancillary services in U.S. electricity markets *Energy Policy* **62** 1031–9
[6] Budischak C, Sewell D, Thomson H, MacH L, Veron D E and Kempton W 2013 Cost-minimized combinations of wind power, solar power and electrochemical storage, powering the grid up to 99.9% of the time *J. Power Sources* **225** 60–74
[7] Winsberg J, Hagemann T, Janoschka T, Hager M D and Schubert U S 2017 Redox-Flow-Batterien: von metallbasierten zu organischen Aktivmaterialien *Angew. Chem.* **129** 702–29
[8] Ravikumar M K, Rathod S, Jaiswal N, Patil S and Shukla A 2016 The renaissance in redox flow batteries *J. Solid State Electrochem.* **21** 2467–88
[9] Leung P, Li X, de León C, Berlouis L, Low C T J and Walsh F C 2012 Progress in redox flow batteries, remaining challenges and their applications in energy storage *RSC Adv.* **2** 10125
[10] Noack J, Roznyatovskaya N, Herr T and Fischer P 2015 Die Chemie der Redox-Flow-Batterien *Angew. Chem.* **127** 9912–47
[11] Deller Z, Jones L A and Maniam S 2021 Aqueous redox flow batteries: how 'green' are the redox active materials? *Green Chem.* **23** 4955–79
[12] Gandini A and Lacerda T M 2015 From monomers to polymers from renewable resources: recent advances *Prog. Polym. Sci.* **48** 1–39
[13] Mukhopadhyay A, Hamel J, Katahira R and Zhu H 2018 Metal-free aqueous flow battery with novel ultrafiltered lignin as electrolyte *ACS Sustain. Chem. Eng.* **6** 5394–400
[14] Fry A J 2017 Computational applications in organic electrochemistry *Curr. Opin. Electrochem.* **2** 67–75
[15] Winget P, Weber E J, Cramer C J and Truhlar D G 2000 Computational electrochemistry: aqueous one-electron oxidation potentials for substituted anilines *Phys. Chem. Chem. Phys.* **2** 1231–9
[16] Ding Y, Zhang C, Zhang L, Zhou Y and Yu G 2018 Molecular engineering of organic electroactive materials for redox flow batteries *Chem. Soc. Rev.* **47** 69–103
[17] Wu J 2006 Density functional theory for chemical engineering: from capillarity to soft materials *AIChE J.* **52** 1169–93
[18] Borioni J L, Puiatti M, Vera D M A and Pierini A B 2017 In search of the best DFT functional for dealing with organic anionic species *Phys. Chem. Chem. Phys.* **19** 9189–98
[19] Isegawa M, Neese F and Pantazis D A 2016 Ionization energies and aqueous redox potentials of organic molecules: comparison of DFT, correlated ab initio theory and pair natural orbital approaches *J. Chem. Theory Comput.* **12** 2272–84
[20] Zhang C, Zhang L, Ding Y, Peng S, Guo X, Zhao Y, He G and Yu G 2018 Progress and prospects of next-generation redox flow batteries *Energy Storage Mater.* **15** 324–50
[21] Sawyer D T 1995 *Electrochemistry for Chemists* (Wiley) p 505
[22] Meites L 1963 *Handbook of Analytical Chemistry* (McGraw-Hill)
[23] Pavlishchuk V V and Addison A W 2000 Conversion constants for redox potentials measured versus different reference electrodes in acetonitrile solutions at 25\textdegreeC *Inorg. Chim. Acta* **298** 97–102
[24] Connelly N G and Geiger W E 1996 Chemical redox agents for organometallic chemistry *Chem. Rev.* **96** 877–910
[25] Batchelor-mcauley C, Li Q, Dapin S M and Compton R G 2010 Voltammetric characterization of DNA intercalators across the full pH range: anthraquinone-2,6-disulfonate and anthraquinone-2-sulfonate *J. Phys. Chem.* B **114** 4094–100
[26] Takaba H, Suzuki T and Nakao S-I 2004 Estimation of diffusion coefficient and permeance of aromatic molecules in silicalite and MgZSM-5 using quantum calculation and dynamic Monte Carlo simulation *Fluid Phase Equilib.* **219** 11–18
[27] Hofmann J D and Schröder D 2019 Which parameter is governing for aqueous redox flow batteries with organic active material? *Chem. Ing. Tech.* **91** 786–94
[28] Costentin C, Robert M and Savéant J-M 2010 Concerted proton-electron transfers: electrochemical and related approaches *Acc. Chem. Res.* **43** 1019–29
[29] Marenich A V, Ho J, Coote M L, Cramer C J and Truhlar D G 2014 Computational electrochemistry: prediction of liquid-phase reduction potentials *Phys. Chem. Chem. Phys.* **16** 15068–106

[30] Briot L, Petit M, Cacciuttolo Q and Pera M-C 2022 Aging phenomena and their modelling in aqueous organic redox flow batteries: a review *J. Power Sources* **536** 231427
[31] Gentil S, Reynard D and Girault H H 2020 Aqueous organic and redox-mediated redox flow batteries: a review *Curr. Opin. Electrochem.* **21** 7–13
[32] Montoto E C *et al* 2016 Redox active colloids as discrete energy storage carriers *J. Am. Chem. Soc.* **138** 13230–7
[33] Barth B A, Imel A, Nelms K M K, Goenaga G A and Zawodzinski T 2022 Microemulsions: breakthrough electrolytes for redox flow batteries *Front. Chem.* **10** 831200
[34] Kravtsova A N, Soldatov M A, Suchkova S A, Butova V V, Bugaev A L, Fain M B and Soldatov A V 2015 Atomic and electronic structure of CdS-based quantum dots *J. Struct. Chem.* **56** 517–22
[35] Zu X, Zhang L, Qian Y, Zhang C and Yu G 2020 Molecular engineering of azobenzene-based anolytes towards high-capacity aqueous redox flow batteries *Angew. Chem., Int. Ed.* **59** 22163–70
[36] Wang X, Chai J, Lashgari A and Jiang J J 2021 Azobenzene-based low-potential anolyte for nonaqueous organic redox flow batteries *ChemElectroChem* **8** 83–89
[37] Li Z, Jiang T, Ali M, Wu C and Chen W 2022 Recent progress in organic species for redox flow batteries *Energy Storage Mater.* **50** 105–38
[38] Gao M, Wang Z, Lek D G and Wang Q 2023 Towards high power density aqueous redox flow batteries *Nano Res. Energy* **2** e9120045
[39] Leung P, Shah A A, Sanz L, Flox C, Morante J R, Xu Q, Mohamed M R, de León C and Walsh F C 2017 Recent developments in organic redox flow batteries: a critical review *J. Power Sources* **360** 243–83
[40] Ghule S, Dash S R, Bagchi S, Joshi K and Vanka K 2022 Predicting the redox potentials of phenazine derivatives using DFT-assisted machine learning *ACS Omega* **7** 11742–55
[41] Cheng L, Assary R S, Qu X, Jain A, Ong S, Rajput N N, Persson K and Curtiss L A 2015 Accelerating electrolyte discovery for energy storage with high-throughput screening *J. Phys. Chem. Lett.* **6** 283–91
[42] Conradie J 2015 A Frontier orbital energy approach to redox potentials *J. Phys.: Conf. Ser.* **633** 012045
[43] Méndez-Hernández D D, Tarakeshwar P, Gust D, Moore T A, Moore A L and Mujica V 2012 Simple and accurate correlation of experimental redox potentials and DFT-calculated HOMO/LUMO energies of polycyclic aromatic hydrocarbons *J. Mol. Model.* **19** 2845–8
[44] Parker V D 1976 Energetics of electrode reactions. II. The relationship between redox potentials, ionization potentials, electron affinities, and solvation energies of aromatic hydrocarbons *J. Am. Chem. Soc.* **98** 98–103
[45] Dandrade B, Datta S, Forrest S, Djurovich P, Polikarpov E and Thompson M 2005 Relationship between the ionization and oxidation potentials of molecular organic semiconductors *Org. Electron.* **6** 11–20
[46] Trasatti S 1986 The absolute electrode potential: an explanatory note (Recommendations 1986) *Pure Appl. Chem.* **58** 955–66
[47] Hammerich O and Speiser B 2015 *Organic Electrochemistry Revised and Expanded* (Taylor and Francis Group) p 1736
[48] Camaioni D M and Schwerdtfeger C A 2005 Comment on "Accurate experimental values for the free energies of hydration of H+, OH−, and H3O+" *J. Phys. Chem.* A **109** 10795–7
[49] Barone V, Cossi M and Tomasi J 1997 A new definition of cavities for the computation of solvation free energies by the polarizable continuum model *J. Chem. Phys.* **107** 3210–21
[50] Kelly C, Cramer C J and Truhlar D G 2005 SM6: a density functional theory continuum solvation model for calculating aqueous solvation free energies of neutrals, ions, and solute-water clusters *J. Chem. Theory Comput.* **1** 1133–52
[51] Klamt A and Schüürmann G 1993 COSMO: a new approach to dielectric screening in solvents with explicit expressions for the screening energy and its gradient *J. Chem. Soc. Perkin Trans.* **2** 799–805
[52] Klamt A, Jonas V, Bürger T and Lohrenz J C W 1998 Refinement and parametrization of COSMO-RS *J. Phys. Chem.* A **102** 5074–85
[53] Bursch M, Mewes J-M, Hansen A and Grimme S 2022 Best-practice DFT protocols for basic molecular computational chemistry *Angew. Chem., Int. Ed.* **61** e202205735
[54] Hopmann K H 2019 How to make your computational paper interesting and have it published *Organometallics* **38** 603–5
[55] Fu Y, Liu L, Yu H-Z, Wang Y-M and Guo Q-X 2005 Quantum-chemical predictions of absolute standard redox potentials of diverse organic molecules and free radicals in acetonitrile *J. Am. Chem. Soc.* **127** 7227–34
[56] Yu J, Shukla G, Fornari R, Arcelus O, Shodiev A, de Silva P and Franco A A 2022 Gaining insight into the electrochemical interface dynamics in an organic redox flow battery with a kinetic Monte Carlo approach *Small* **18** 2107720
[57] Steinmann S N, Wodrich M D and Corminboeuf C 2010 Overcoming systematic DFT errors for hydrocarbon reaction energies *Theor. Chem. Acc.* **127** 429–42
[58] Zhao Y and Truhlar D G 2008 Density functionals with broad applicability in chemistry *Acc. Chem. Res.* **41** 157–67
[59] Autschbach J and Srebro M 2014 Delocalization error and "functional tuning" in Kohn–Sham calculations of molecular properties *Acc. Chem. Res.* **47** 2592–602
[60] Jónsson E and Johansson P 2015 Electrochemical oxidation stability of anions for modern battery electrolytes: a CBS and DFT study *Phys. Chem. Chem. Phys.* **17** 3697–703
[61] Duque-Prata A, Pinto T, Serpa C and Caridade P 2022 Performance of functionals and basis sets in DFT calculation of organic compounds redox potentials of nitrile alkenes and aromatic molecules using density functional theory *ChemistrySelect* **8** e202300205
[62] Yamamoto Y, Diaz C M, Basurto L, Jackson K A, Baruah T and Zope R R 2019 Fermi-Löwdin orbital self-interaction correction using the strongly constrained and appropriately normed meta-GGA functional *J. Chem. Phys.* **151** 154105
[63] Klimeš J and Michaelides A 2012 Perspective: advances and challenges in treating van der Waals dispersion forces in density functional theory *J. Chem. Phys.* **137** 120901
[64] Gillan M J, Alfè D and Michaelides A 2016 Perspective: how good is DFT for water? *J. Chem. Phys.* **144** 130901
[65] Bryenton K R, Adeleke A A, Dale S G and Johnson E R 2022 Delocalization error: the greatest outstanding challenge in density-functional theory *WIREs Comput. Mol. Sci.* **13** e1631
[66] Bannwarth C, Caldeweyher E, Ehlert S, Hansen A, Pracht P, Seibert J, Spicher S and Grimme S 2020 Extended tight-binding quantum chemistry methods *WIREs Comput. Mol. Sci.* **11** e1493
[67] Bannwarth C, Ehlert S and Grimme S 2019 GFN2-xTB—an accurate and broadly parametrized self-consistent tight-binding quantum chemical method with multipole electrostatics and density-dependent dispersion contributions *J. Chem. Theory Comput.* **15** 1652–71

[68] Zhang Q, Khetan A and Er S 2020 Comparison of computational chemistry methods for the discovery of quinone-based electroactive compounds for energy storage *Sci. Rep.* **10** 22149
[69] Guerard J J and Arey J S 2013 Critical evaluation of implicit solvent models for predicting aqueous oxidation potentials of neutral organic compounds *J. Chem. Theory Comput.* **9** 5046–58
[70] Sterling C M and Bjornsson R 2018 Multistep explicit solvation protocol for calculation of redox potentials *J. Chem. Theory Comput.* **15** 52–67
[71] Weaver M N, Janicki S Z and Petillo A 2001 *Ab initio* calculation of inner-sphere reorganization energies of arenediazonium ion couples *J. Org. Chem.* **66** 1138–45
[72] Mikhailov M N, Mendkovich A S, Kuzminsky M B and Rusakov A I 2007 A multiconfigurational study of anion-radical and dianion of 1,3-dinitrobenzene *J. Mol. Struct.* **847** 103–6
[73] Ren W, Lukens W W, Zi G, Maron L and Walter M D 2013 Is the bipyridyl thorium metallocene a low-valent thorium complex? A combined experimental and computational study *Chem. Sci.* **4** 1168
[74] Rosenzweig M W, Heinemann F W, Maron L and Meyer K 2017 Molecular and electronic structures of eight-coordinate uranium bipyridine complexes: a rare example of a Bipy2—ligand coordinated to a U4+ ion *Inorg. Chem.* **56** 2792–800
[75] Ehrmaier J, Picconi D, Karsili T N V and Domcke W 2017 Photodissociation dynamics of the pyridinyl radical: time-dependent quantum wave-packet calculations *J. Chem. Phys.* **146** 124304
[76] Grimme S and Schreiner R 2017 Computational chemistry: the fate of current methods and future challenges *Angew. Chem., Int. Ed.* **57** 4170–6
[77] Toulouse J, Assaraf R and Umrigar C J 2016 Introduction to the variational and diffusion Monte Carlo methods *Advances in Quantum Chemistry* (Elsevier) pp 285–314
[78] Booth G H and Alavi A 2010 Approaching chemical accuracy using full configuration-interaction quantum Monte Carlo: a study of ionization potentials *J. Chem. Phys.* **132** 174104
[79] Dupuy N, Bouaouli S, Mauri F, Sorella S and Casula M 2015 Vertical and adiabatic excitations in anthracene from quantum Monte Carlo: constrained energy minimization for structural and electronic excited-state properties in the JAGP ansatz *J. Chem. Phys.* **142** 214109
[80] Rudshteyn B, Weber J L, Coskun D, Devlaminck A, Zhang S, Reichman D R, Shee J and Friesner R A 2022 Calculation of metallocene ionization potentials via auxiliary field quantum Monte Carlo: toward benchmark quantum chemistry for transition metals *J. Chem. Theory Comput.* **18** 2845–62
[81] Kestner N R and Combariza J E 2007 Basis set superposition errors: theory and practice *Reviews in Computational Chemistry* (Wiley) pp 99–132
[82] Bernardi F, Bottoni A and Garavelli M 2002 Exploring organic chemistry with DFT: radical, organo-metallic, and bio-organic applications *Quant. Struct.* **21** 128–48
[83] Chéron N, Jacquemin D and Fleurat-Lessard P 2012 A qualitative failure of B3LYP for textbook organic reactions *Phys. Chem. Chem. Phys.* **14** 7170
[84] Wenthold G and Winter A H 2018 Nucleophilic addition to singlet diradicals: homosymmetric diradicals *J. Org. Chem.* **83** 12390–6
[85] Saito T, Nishihara S, Yamanaka S, Kitagawa Y, Kawakami T, Yamada S, Isobe H, Okumura M and Yamaguchi K 2011 Symmetry and broken symmetry in molecular orbital description of unstable molecules IV: comparison between single- and multi-reference computational results for antiaromtic molecules *Theor. Chem. Acc.* **130** 749–63
[86] Vosskötter S, Konieczny P, Marian C M and Weinkauf R 2015 Towards an understanding of the singlet–triplet splittings in conjugated hydrocarbons: azulene investigated by anion photoelectron spectroscopy and theoretical calculations *Phys. Chem. Chem. Phys.* **17** 23573–81
[87] Armstrong C G and Toghill K E 2018 Stability of molecular radicals in organic non-aqueous redox flow batteries: a mini review *Electrochem. Commun.* **91** 19–24
[88] Janoschka T, Martin N, Hager M D and Schubert U S 2016 An aqueous redox-flow battery with high capacity and power: the TEMPTMA/MV system *Angew. Chem., Int. Ed.* **55** 14427–30
[89] Wedege K, Bae D, Dražević E, Mendes A, Vesborg C K and Bentien A 2018 Unbiased, complete solar charging of a neutral flow battery by a single Si photocathode *RSC Adv.* **8** 6331–40
[90] Wylie L, Blesch T, Freeman R, Hatakeyama-Sato K, Oyaizu K, Yoshizawa-Fujita M and Izgorodina E I 2020 Reversible reduction of the TEMPO radical: one step closer to an all-organic redox flow battery *ACS Sustain. Chem. Eng.* **8** 17988–96
[91] Winsberg J, Stolze C, Muench S, Liedl F, Hager M D and Schubert U S 2016 TEMPO/phenazine combi-molecule: a redox-active material for symmetric aqueous redox-flow batteries *ACS Energy Lett.* **1** 976–80
[92] Nutting J E, Rafiee M and Stahl S S 2018 Tetramethylpiperidine N-oxyl (TEMPO), phthalimide N-oxyl (PINO), and related n-oxyl species: electrochemical properties and their use in electrocatalytic reactions *Chem. Rev.* **118** 4834–85
[93] Krishna M C, Grahame D A, Samuni A, Mitchell J B and Russo A 1992 Oxoammonium cation intermediate in the nitroxide-catalyzed dismutation of superoxide. *Proc. Natl Acad. Sci.* **89** 5537–41
[94] Hu S, Wang L, Yuan X, Xiang Z, Huang M, Luo P, Liu Y, Fu Z and Liang Z 2021 Viologen-decorated TEMPO for neutral aqueous organic redox flow batteries *Energy Mater. Adv.* **2021** 1–8
[95] Mao S-C, Qu J-Q and Zheng K-C 2012 Theoretical study on electronic gain-and-loss properties of TEMPO and its derivates in charge/discharge processes *Chin. J. Chem. Phys.* **25** 161–8
[96] Mendkovich A S, Luzhkov V B, Syroeshkin M A, Sen V D, Khartsii D I and Rusakov A I 2017 Influence of the nature of solvent and substituents on the oxidation potential of 2,2,6,6-tetramethylpiperidine 1-oxyl derivatives *Russ. Chem. Bull.* **66** 683–9
[97] Hodgson J L, Namazian M, Bottle S E and Coote M L 2007 One-electron oxidation and reduction potentials of nitroxide antioxidants: a theoretical study *J. Phys. Chem. A* **111** 13595–605
[98] Zens C, Friebe C, Schubert U S, Richter M and Kupfer S 2022 Tailored charge transfer kinetics in precursors for organic radical batteries—a joint synthetic-theoretical approach *ChemSusChem* **16** e202201679
[99] D'Amore M, Improta R and Barone V 2003 Conformational behavior and magnetic properties of a nitroxide amino acid derivative in vacuo and in aqueous solution *J. Phys. Chem.* A **107** 6264–9
[100] Nambafu G S 2021 Organic molecules as bifunctional electroactive materials for symmetric redox flow batteries: a mini review *Electrochem. Commun.* **127** 107052
[101] Li M, Case J and Minteer S D 2021 Bipolar redox-active molecules in non-aqueous organic redox flow batteries: status and challenges *ChemElectroChem* **8** 1215–32

[102] Rhodes Z, Cabrera-Pardo J R, Li M and Minteer S D 2020 Electrochemical advances in non-aqueous redox flow batteries *Isr. J. Chem.* **61** 101–12
[103] Oxgaard J and Wiest O 2001 Symmetry, radical ions, and butadienes: exploring the limits of density functional theory *J. Phys. Chem.* A **105** 8236–40
[104] Steen J S, Nuismer J L, Eiva V, Wiglema A E T, Daub N, Hjelm J and Otten E 2022 Blatter radicals as bipolar materials for symmetrical redox-flow batteries *J. Am. Chem. Soc.* **144** 5051–8
[105] Constantinides C, Berezin A, Zissimou G, Manoli M, Leitus G and Koutentis P A 2016 The suppression of columnar pi-stacking in 3-adamantyl-1-phenyl-1,4-dihydrobenzo[e][1,2,4]triazin-4-yl *Molecules* **21** 636
[106] Morgan I S, Peuronen A, Hänninen M M, Reed R W, Clérac R and Tuononen H M 2013 1-phenyl-3-(pyrid-2-yl)benzo[e][1,2,4]triazinyl: the first "Blatter radical" for coordination chemistry *Inorg. Chem.* **53** 33–35
[107] Rawson J 1999 Benzo-fused dithiazolyl radicals: from chemical curiosities to materials chemistry *Coord. Chem. Rev.* **189** 135–68
[108] Boere R T, Moock K H and Parvez M 1994 Electrochemical evidence for the existence of three stable oxidation states for heterocycles of the type XC6H4CN2E2 (E = S, Se). X-ray crystal structure of the dimer with X = Cl, E = S *Z. Anorg. Allg. Chem.* **620** 1589–98
[109] Aherne C M, Banister A J, Gorrell I B, Hansford M I, Hauptman Z V, Luke A W and Rawson J M 1993 Electrochemical studies of some dithiadiazolylium cations evidence for the dithiadiazolide anion, [PhCNSSN] *J. Chem. Soc. Dalton Trans.* **967** 967–72
[110] Alberola A, Clements O, Collis R J, Cubbitt L, Grant C M, Less R J, Oakley R T, Rawson J M, Reed R W and Robertson C M 2008 Polymorphism in a π-stacked 1,3,2-dithiazolyl radical: pyridyl-1,3,2-dithiazolyl *Cryst. Growth Des.* **8** 155–61
[111] Oakley R T, Reed R W, Robertson C M and Richardson J F 2005 Naphthalene-1,2,3-dithiazolyl and its selenium-containing variants *Inorg. Chem.* **44** 1837–45
[112] Kaczmarek L A, Zaichenko A and Mollenhauer D n.d. Investigation of reduction potentials and structure of dithiazolyle- and dithiadiazolyl-based radicals, anions and cations submitted
[113] Huang J *et al* 2016 The lightest organic radical cation for charge storage in redox flow batteries *Sci. Rep.* **6** 32102
[114] Wang X 2018 Study of tetraethylammonium bis(trifluoromethylsulfonyl)imide as a supporting electrolyte for an all-organic redox flow battery using benzophenone and 1,4-di-tert-butyl-2,5-dimethoxybenzene as active species *Int. J. Electrochem. Sci.* **13** 6676–83
[115] Moon Y and Han Y-K 2016 Computational screening of organic molecules as redox active species in redox flow batteries *Curr. Appl. Phys.* **16** 939–43
[116] Doan H A, Agarwal G, Qian H, Counihan M J, Rodríguez-López J, Moore J S and Assary R S 2020 Quantum chemistry-informed active learning to accelerate the design and discovery of sustainable energy storage materials *Chem. Mater.* **32** 6338–46
[117] Assary R S, Zhang L, Huang J and Curtiss L A 2016 Molecular level understanding of the factors affecting the stability of dimethoxy benzene catholyte candidates from first-principles investigations *J. Phys. Chem.* C **120** 14531–8
[118] Gilroy J B, McKinnon S D J, Koivisto B D and Hicks R G 2007 Electrochemical studies of verdazyl radicals *Org. Lett.* **9** 4837–40
[119] Neugebauer F A, Fischer H and Siegel R 1988 6-Oxo- und 6-thioxoverdazyle *Chem. Ber.* **121** 815–22
[120] Kuhn R and Trischmann H 1964 Ueber Verdazyle, eine neue Klasse cyclischer N-haltiger Radikale *Mon. Chem.* **95** 457–79
[121] Kunz S, van Rensburg M J, Pietruschka D S, Achazi A J, Emmel D, Kerner F, Mollenhauer D, Wegner H A and Schröder D 2022 Unraveling the electrochemistry of verdazyl species in acidic electrolytes for the application in redox flow batteries *Chem. Mater.* **34** 10424–34
[122] Koivisto B D and Hicks R G 2005 The magnetochemistry of verdazyl radical-based materials *Coord. Chem. Rev.* **249** 2612–30
[123] Tanaseichuk B S, Tomilin O B, Pryanichnikova M K, Tsebulaeva Y V and Boyarkina O V 2017 Reaction of 1,5-diphenyl-3-arylverdazyles with CH-acids *Russ. J. Organ. Chem.* **53** 764–8
[124] Charlton G D, Barbon S M, Gilroy J B and Dyker C A 2019 A bipolar verdazyl radical for a symmetric all-organic redox flow-type battery *J. Energy Chem.* **34** 52–56
[125] Korshunov A, Milner M J, Grünebaum M, Studer A, Winter M and Cekic-Laskovic I 2020 An oxo-verdazyl radical for a symmetrical non-aqueous redox flow battery *J. Mater. Chem.* A **8** 22280–91
[126] Steen J S, de Vries F, Hjelm J and Otten E 2022 Bipolar verdazyl radicals for symmetrical batteries: properties and stability in all states of charge *ChemPhysChem* **24** e202200779
[127] Liu F, Proynov E, Yu J-G, Furlani T R and Kong J 2012 Comparison of the performance of exact-exchange-based density functional methods *J. Chem. Phys.* **137** 114104
[128] Harding L B, Klippenstein S J and Jasper A W 2007 Ab initio methods for reactive potential surfaces *Phys. Chem. Chem. Phys.* **9** 4055
[129] Izgorodina E I, Brittain D R B, Hodgson J L, Krenske E H, Lin C Y, Namazian M and Coote M L 2007 Should contemporary density functional theory methods be used to study the thermodynamics of radical reactions? *J. Phys. Chem.* A **111** 10754–68
[130] Szalay G, Müller T, Gidofalvi G, Lischka H and Shepard R 2011 Multiconfiguration self-consistent field and multireference configuration interaction methods and applications *Chem. Rev.* **112** 108–81
[131] Gagliardi L, Truhlar D G, Manni G L, Carlson R K, Hoyer C E and Bao J L 2016 Multiconfiguration pair-density functional theory: a new way to treat strongly correlated systems *Acc. Chem. Res.* **50** 66–73
[132] Huskinson B, Marshak M, Suh C, Er S, Gerhardt M R, Galvin C J, Chen X, Aspuru-Guzik A, Gordon R G and Aziz M J 2014 A metal-free organic–inorganic aqueous flow battery *Nature* **505** 195–8
[133] Xu Y, Wen Y, Cheng J, Cao G and Yang Y 2009 Study on a single flow acid Cd–chloranil battery *Electrochem. Commun.* **11** 1422–4
[134] Pahlevaninezhad M, Leung P, Velasco Q, Pahlevani M, Walsh F C, Roberts E L and de León C 2021 A nonaqueous organic redox flow battery using multi-electron quinone molecules *J. Power Sources* **500** 229942
[135] Bauer S, Namyslo J C, Kaufmann D E and Turek T 2020 Evaluation of options and limits of aqueous all-quinone-based organic redox flow batteries *J. Electrochem. Soc.* **167** 110522
[136] Ding Y, Li Y and Yu G 2016 Exploring bio-inspired quinone-based organic redox flow batteries: a combined experimental and computational study *Chem* **1** 790–801
[137] Tabor D, Gómez-Bombarelli R, Tong L, Gordon R G, Aziz M J and Aspuru-Guzik A 2019 Mapping the frontiers of quinone stability in aqueous media: implications for organic aqueous redox flow batteries *J. Mater. Chem.* A **7** 12833–41
[138] Leung P, Martin T, Xu Q, Flox C, Mohamad M R, Palma J, Rodchanarowan A, Zhu X, Xing W W and Shah A A 2021 A new aqueous all-organic flow battery with high cell voltage in acidic electrolytes *Appl. Energy* **282** 116058
[139] Siddiqui S A 2020 In silico investigation for the design of redox based molecular switch *Russ. J. Phys. Chem.* A **94** 1422–6
[140] Kim H, Goodson T and Zimmerman M 2016 Achieving accurate reduction potential predictions for anthraquinones in water and aprotic solvents: effects of inter- and intramolecular H-bonding and ion pairing *J. Phys. Chem.* C **120** 22235–47

[141] Hofmann J D, Pfanschilling F L, Krawczyk N, Geigle P, Hong L, Schmalisch S, Wegner H A, Mollenhauer D, Janek J and Schröder D 2018 Quest for organic active materials for redox flow batteries: 2,3-diaza-anthraquinones and their electrochemical properties *Chem. Mater.* **30** 762–74
[142] Gallmetzer J M, Kröll S, Werner D, Wielend D, Irimia-Vladu M, Portenkirchner E, Sariciftci N S and Hofer T S 2022 Anthraquinone and its derivatives as sustainable materials for electrochemical applications—a joint experimental and theoretical investigation of the redox potential in solution *Phys. Chem. Chem. Phys.* **24** 16207–19
[143] Chen R 2020 Redox flow batteries for energy storage: recent advances in using organic active materials *Curr. Opin. Electrochem.* **21** 40–45
[144] Ruan W, Mao J and Chen Q 2021 Redox flow batteries toward more soluble anthraquinone derivatives *Curr. Opin. Electrochem.* **29** 100748
[145] Zhang S, Li X and Chu D 2016 An organic electroactive material for flow batteries *Electrochim. Acta* **190** 737
[146] Wu M, Bahari M, Jing Y, Amini K, Fell E M, George T Y, Gordon R G and Aziz M J 2022 Highly stable, low redox potential quinone for aqueous flow batteries *Batter. Supercaps* **5**
[147] Zhang J, Huang J, Robertson L A, Shkrob I A and Zhang L 2018 Comparing calendar and cycle life stability of redox active organic molecules for nonaqueous redox flow batteries *J. Power Sources* **397** 214–22
[148] Kim K C, Liu T, Jung K H, Lee S W and Jang S S 2019 Unveiled correlations between electron affinity and solvation in redox potential of quinone-based sodium-ion batteries *Energy Storage Mater.* **19** 242–50
[149] Er S, Suh C, Marshak M and Aspuru-Guzik A 2015 Computational design of molecules for an all-quinone redox flow battery *Chem. Sci.* **6** 885–93
[150] Schwan S, Schröder D, Wegner H A, Janek J and Mollenhauer D 2020 Substituent pattern effects on the redox potentials of quinone-based active materials for aqueous redox flow batteries *ChemSusChem* **13** 5480–8
[151] Bachman J E, Curtiss L A and Assary R S 2014 Investigation of the redox chemistry of anthraquinone derivatives using density functional theory *J. Phys. Chem.* A **118** 8852–60
[152] Chen L 2017 First principles design of anthraquinone derivatives in redox flow batteries *Int. J. Electrochem. Sci.* **12** 10433–46
[153] Zhigalko M V, Shishkin O V, Gorb L and Leszczynski J 2004 Out-of-plane deformability of aromatic systems in naphthalene, anthracene and phenanthrene *J. Mol. Struct.* **693** 153–9
[154] Li J, Xu H, Wang J, Wang Y, Lu D, Liu J and Wu J 2021 Theoretical insights on the hydration of quinones as catholytes in aqueous redox flow batteries *Chin. J. Chem. Eng.* **37** 72–78
[155] Wass J R T J, Ahlberg E, Panas I and Schiffrin D J 2006 Quantum chemical modeling of the reduction of quinones *J. Phys. Chem. A* **110** 2005–20
[156] Zhang J, Zhang H, Wu T, Wang Q and van der Spoel D 2017 Comparison of implicit and explicit solvent models for the calculation of solvation free energy in organic solvents *J. Chem. Theory Comput.* **13** 1034–43
[157] Gaudin T and Aubry J-M 2022 Prediction of Pourbaix diagrams of quinones for redox flow battery by COSMO-RS *J. Energy Storage* **49** 104152
[158] Hofmann J D, Schmalisch S, Schwan S, Hong L, Wegner H A, Mollenhauer D, Janek J and Schröder D 2020 Tailoring dihydroxyphthalazines to enable their stable and efficient use in the catholyte of aqueous redox flow batteries *Chem. Mater.* **32** 3427–38
[159] Sevov C S, Brooner R E M, Chénard E, Assary R S, Moore J S, Rodríguez-López J and Sanford M S 2015 Evolutionary design of low molecular weight organic anolyte materials for applications in nonaqueous redox flow batteries *J. Am. Chem. Soc.* **137** 14465–72
[160] Wang H, Huang X, Shen R, Rui L and Fu Y 2010 Theoretical study of one-electron redox potentials of some NADH model compounds *Chin. J. Chem.* **28** 72–80
[161] DeBruler C, Hu B, Moss J, Liu X, Luo J, Sun Y and Liu T L 2017 Designer two-electron storage viologen anolyte materials for neutral aqueous organic redox flow batteries *Chem* **3** 961–78
[162] Beh E S, Porcellinis D D, Gracia R L, Xia K T, Gordon R G and Aziz M J 2017 A neutral pH aqueous organic- organometallic redox flow battery with extremely high capacity retention *ACS Energy Lett.* **2** 639–44
[163] Korshunov A, Gibalova A, Grünebaum M, Ravoo B J, Winter M and Cekic-Laskovic I 2021 Host-guest interactions enhance the performance of viologen electrolytes for aqueous organic redox flow batteries *Batter. Supercaps* **4** 923–8
[164] Shimizu A, Ishizaki Y, Horiuchi S, Hirose T, Matsuda K, Sato H and Yoshida J-I 2020 HOMO–LUMO energy-gap tuning of π-conjugated zwitterions composed of electron-donating anion and electron-accepting cation *J. Org. Chem.* **86** 770–81
[165] Chen C, Zhang S, Zhu Y, Qian Y, Niu Z, Ye J, Zhao Y and Zhang X 2018 Pyridyl group design in viologens for anolyte materials in organic redox flow batteries *RSC Adv.* **8** 18762–70
[166] Liu Y, Li Y, Zuo P, Chen Q, Tang G, Sun P, Yang Z and Xu T 2020 Screening viologen derivatives for neutral aqueous organic redox flow batteries *ChemSusChem* **13** 2245–9
[167] Alkhayri F and Dyker C A 2020 A two-electron bispyridinylidene anolyte for non-aqueous organic redox flow batteries *J. Electrochem. Soc.* **167** 160548
[168] Chai J, Lashgari A, Wang X and Jiang J 2020 Extending the redox potentials of metal-free anolytes: towards high energy density redox flow batteries *J. Electrochem. Soc.* **167** 100556
[169] Kannappan R, Bucher C, Saint-Aman E, Moutet J-C, Milet A, Oltean M, Métay E, Pellet-Rostaing S, Lemaire M and Chaix C 2010 Viologen-based redox-switchable anion-binding receptors *New J. Chem.* **34** 1373
[170] Villagrán C, Banks C E, Pitner W R, Hardacre C and Compton R G 2005 Electroreduction of N-methylphthalimide in room temperature ionic liquids under insonated and silent conditions *Ultrason. Sonochem.* **12** 423–8
[171] Li Z, Li S, Liu S, Huang K, Fang D, Wang F and Peng S 2011 Electrochemical properties of an all-organic redox flow battery using 2,2,6,6-tetramethyl-1-piperidinyloxy and N-methylphthalimide *Electrochem. Solid-State Lett.* **14** A171
[172] Li Z and Lu Y-C 2018 Redox flow batteries: want more electrons? Go organic! *Chem* **4** 2020–1
[173] Lee M, Hong J, Lee B, Ku K, Lee S, Park C B and Kang K 2017 Multi-electron redox phenazine for ready-to-charge organic batteries *Green Chem.* **19** 2980–5
[174] Hollas A, Wei X, Murugesan V, Nie Z, Li B, Reed D, Liu J, Sprenkle V and Wang W 2018 A biomimetic high-capacity phenazine-based anolyte for aqueous organic redox flow batteries *Nat. Energy* **3** 508–14
[175] Wang C, Li X, Yu B, Wang Y, Yang Z, Wang H, Lin H, Ma J, Li G and Jin Z 2020 Molecular design of fused-ring phenazine derivatives for long-cycling alkaline redox flow batteries *ACS Energy Lett.* **5** 411–7
[176] Xu J, Pang S, Wang X, Wang P and Ji Y 2021 Ultrastable aqueous phenazine flow batteries with high capacity operated at elevated temperatures *Joule* **5** 2437–49

[177] Wellala N N, Hollas A, Duanmu K, Murugesan V, Zhang X, Feng R, Shao Y and Wang W 2021 Decomposition pathways and mitigation strategies for highly-stable hydroxyphenazine flow battery anolytes *J. Mater. Chem.* A **9** 21918–28
[178] Huang B, Kang H, Zhao X-L, Yang H-B and Shi X 2022 Redox properties of N,N′-disubstituted dihydrophenazine and dihydrodibenzo[a,c]phenazine: the first isolation of their crystalline radical cations and dications *Cryst. Growth Des.* **22** 3587–93
[179] Paduszek B and Kalinowski M K 1983 Redox behaviour of phenothiazine and phenazine in organic solvents *Electrochim. Acta* **28** 639–42
[180] Castro K *et al* 2016 Incremental tuning up of fluorous phenazine acceptors *Chem. Eur. J.* **22** 3930–6
[181] Zhang W, Chen Y, Wu T-R, Xia X, Xu J, Chen Z, Cao J and Wu D-Y 2022 Computational design of phenazine derivative molecules as redox-active electrolyte materials in alkaline aqueous organic flow batteries *New J. Chem.* **46** 11662–8
[182] de la Cruz C, Molina A, Patil N, Ventosa E, Marcilla R and Mavrandonakis A 2020 New insights into phenazine-based organic redox flow batteries by using high-throughput DFT modelling *Sustain. Energy Fuels* **4** 5513–21
[183] Assary R S, Brushett F R and Curtiss L A 2014 Reduction potential predictions of some aromatic nitrogen-containing molecules *RSC Adv.* **4** 57442–51
[184] Fornari R, Mesta M, Hjelm J, Vegge T and Silva D 2020 Molecular engineering strategies for symmetric aqueous organic redox flow batteries *ACS Mater. Lett.* **2** 239–46
[185] Chen J-J, Chen W, He H, Li D-B, Li W-W, Xiong L and Yu H-Q 2012 Manipulation of microbial extracellular electron transfer by changing molecular structure of phenazine-type redox mediators *Environ. Sci. Technol.* **47** 1033–9
[186] Nakagawa R and Nishina Y 2021 Simulating the redox potentials of unexplored phenazine derivatives as electron mediators for biofuel cells *J. Phys. Energy* **3** 034008
[187] Miao L, Liu L, Zhang K and Chen J 2020 Molecular design strategy for high-redox-potential and poorly soluble n-type phenazine derivatives as cathode materials for lithium batteries *ChemSusChem* **13** 2337–44
[188] Zhang L, Qian Y, Feng R, Ding Y, Zu X, Zhang C, Guo X, Wang W and Yu G 2020 Reversible redox chemistry in azobenzene-based organic molecules for high-capacity and long-life nonaqueous redox flow batteries *Nat. Commun.* **11** 3843
[189] Xu D, Zhang C, Zhen Y, Zhao Y and Li Y 2021 A high-rate nonaqueous organic redox flow battery *J. Power Sources* **495** 229819
[190] Fliegl H, Köhn A, Hättig C and Ahlrichs R 2003 *Ab initio* calculation of the vibrational and electronic spectra of trans- and cis-azobenzene *J. Am. Chem. Soc.* **125** 9821–7
[191] Wang X, Chai J, Devi N, Lashgari A, Chaturvedi A and Jiang J 2021 Two-electron-active tetracyanoethylene for nonaqueous redox flow batteries *J. Mater. Chem.* A **9** 13867–73
[192] Huang J, Yang Z, Vijayakumar M, Duan W, Hollas A, Pan B, Wang W, Wei X and Zhang L 2018 A two-electron storage nonaqueous organic redox flow battery *Adv. Sustain. Syst.* **2** 1700131
[193] Yan Y, Robinson S G, Vaid T, Sigman M S and Sanford M S 2021 Simultaneously enhancing the redox potential and stability of multi-redox organic catholytes by incorporating cyclopropenium substituents *J. Am. Chem. Soc.* **143** 13450–9
[194] Rawashdeh A M M 2005 Computing the redox potentials of phenothiazine and N-methylphenothiazine *Abhath Al-Yarmouk "Basic Science and Engineering"* pp 195–208
[195] Zhang W-W, Mao W-L, Hu Y-X, Tian Z-Q, Wang Z-L and Meng Q-J 2009 Phenothiazine-anthraquinone donor-acceptor molecules: synthesis, electronic properties and DFT-TDDFT computational study *J. Phys. Chem.* A **113** 9997–10004
[196] Chiykowski V A, Lam B, Du C and Berlinguette C 2017 On how electron density affects the redox stability of phenothiazine sensitizers on semiconducting surfaces *Chem. Commun.* **53** 2547–50
[197] Zhang C, Niu Z, Peng S, Ding Y, Zhang L, Guo X, Zhao Y and Yu G 2019 Phenothiazine-based organic catholyte for high-capacity and long-life aqueous redox flow batteries *Adv. Mater.* **31** 1901052
[198] Casselman M D, Kaur A, Narayana K A, Elliott C F, Risko C and Odom S A 2015 The fate of phenothiazine-based redox shuttles in lithium-ion batteries *Phys. Chem. Chem. Phys.* **17** 6905–12
[199] Kowalski J A *et al* 2017 A stable two-electron-donating phenothiazine for application in nonaqueous redox flow batteries *J. Mater. Chem. A* **5** 24371–9
[200] Huang J, Duan W, Zhang J, Shkrob I A, Assary R S, Pan B, Liao C, Zhang Z, Wei X and Zhang L 2018 Substituted thiadiazoles as energy-rich anolytes for nonaqueous redox flow cells *J. Mater. Chem.* A **6** 6251–4
[201] Yan Y, Zhang L, Walser-Kuntz R, Vogt D B, Sigman M S, Yu G and Sanford M S 2022 Benzotriazoles as low-potential anolytes for non-aqueous redox flow batteries *Chem. Mater.* **34** 10594–605
[202] Zając D, Honisz D, Łapkowski M and Sołoducho J 2021 2,1,3-benzothiadiazole small donor molecules: a DFT study, synthesis, and optoelectronic properties *Molecules* **26** 1216
[203] Rietsch P, Sobottka S, Hoffmann K, Popov A A, Hildebrandt P, Sarkar B, Resch-Genger U and Eigler S 2020 Between aromatic and quinoid structure: a symmetrical UV to Vis/NIR benzothiadiazole redox switch *Chem. Eur. J.* **26** 17361–5
[204] Axelsson M, Marchiori C F N, Huang P, Araujo C M and Tian H 2021 Small organic molecule based on benzothiadiazole for electrocatalytic hydrogen production *J. Am. Chem. Soc.* **143** 21229–33
[205] Howard J D, Assary R S and Curtiss L A 2020 Insights into the interaction of redox active organic molecules and solvents with the pristine and defective graphene surfaces from density functional theory *J. Phys. Chem.* C **124** 2799–805
[206] Pelzer K M, Cheng L and Curtiss L A 2017 Effects of functional groups in redox-active organic molecules: a high-throughput screening approach *J. Phys. Chem.* C **121** 237–45
[207] Antoni W and Hansmann M M 2018 Pyrylenes: a new class of tunable, redox-switchable, photoexcitable pyrylium–carbene hybrids with three stable redox-states *J. Am. Chem. Soc.* **140** 14823–35
[208] Caro B, Guen F R-L, Sénéchal-Tocquer M-C, Prat V and Vaissermann J 1997 Synthesis, structure and reactivity of acetylenic $Co_2(CO)_6$ pyrylium salts. Electronic influence of the $Co_2(CO)_6$ acetylenic fragment *J. Organomet. Chem.* **543** 87–92
[209] Saeva F D and Olin G R 1980 Electron-donating properties of oxygen vs. sulfur. Redox potentials for some pyrylium and thiapyrylium salts *J. Am. Chem. Soc.* **102** 299–303
[210] Ismail M I 1991 Polarographic reduction of pyrylium salts *Tetrahedron* **47** 1957–64
[211] Milov A A, Starikov A G, Gridin M K and Minyaev R M 2007 Effect of the counterion on the steric and electronic structure of pyrylium cation *Russ. J. Gen. Chem.* **77** 1373–85
[212] Müller C *et al* 2007 Donor-functionalized polydentate pyrylium salts and phosphinines: synthesis, structural characterization, and photophysical properties *Chem. Eur. J.* **13** 4548–59
[213] Parreira R L T and Galembeck S E 2006 Computational study of pyrylium cation–water complexes: hydrogen bonds, resonance effects, and aromaticity *J. Mol. Struct.* **760** 59–73
[214] Ding Y, Zhao Y, Li Y, Goodenough J B and Yu G 2017 A high-performance all-metallocene-based, non-aqueous redox flow battery *Energy Environ. Sci.* **10** 491–7

[215] Calborean A, Buimaga-Iarinca L and Graur F 2015 DFT charge transfer of hybrid molecular ferrocene/Si structures *Phys. Scr.* **90** 055803
[216] Pham-Truong T N, Wang Q, Ghilane J and Randriamahazaka H 2020 Recent advances in the development of organic and organometallic redox shuttles for lithium-ion redox flow batteries *ChemSusChem* **13** 2142–59
[217] Huang Y, Gu S, Yan Y and Li S F Y 2015 Nonaqueous redox-flow batteries: features, challenges, and prospects *Curr. Opin. Chem. Eng.* **8** 105–13
[218] Drosou M, Mitsopoulou C A and Pantazis D A 2021 Spin-state energetics of manganese spin crossover complexes: comparison of single-reference and multi-reference ab initio approaches *Polyhedron* **208** 115399
[219] Milko P and Iron M A 2013 On the innocence of bipyridine ligands: how well do DFT functionals fare for these challenging spin systems? *J. Chem. Theory Comput.* **10** 220–35
[220] Shee J, Loipersberger M, Hait D, Lee J and Head-Gordon M 2021 Revealing the nature of electron correlation in transition metal complexes with symmetry breaking and chemical intuition *J. Chem. Phys.* **154** 194109
[221] Kucharyson J F, Cheng L, Tung S O, Curtiss L A and Thompson L T 2017 Predicting the potentials, solubilities and stabilities of metal-acetylacetonates for non-aqueous redox flow batteries using density functional theory calculations *J. Mater. Chem.* A **5** 13700–9
[222] Carino E V, Staszak-Jirkovsky J, Assary R S, Curtiss L A, Markovic N M and Brushett F R 2016 Tuning the stability of organic active materials for nonaqueous redox flow batteries via reversible, electrochemically mediated Li+ coordination *Chem. Mater.* **28** 2529–39